HHS Public Access

Author manuscript

J Comp Neurol. Author manuscript; available in PMC 2019 June 01.

Published in final edited form as:

J Comp Neurol. 2018 June 01; 526(8): 1287–1306. doi:10.1002/cne.24407.

Neurotransmitter Diversity In Pre-Synaptic Terminals Located in the Parvicellular Neuroendocrine Paraventricular Nucleus of the Rat and Mouse Hypothalamus

Caroline S. Johnson[1], **Jaideep S. Bains**[2], and **Alan G. Watts**[1]

[1]The Department of Biological Sciences, USC Dornsife College of Letters, Arts, and Sciences, and Neuroscience, Graduate Program, University of Southern California, Los Angeles, USA

[2]Hotchkiss Brain Institute and Dept. of Physiology and Pharmacology, University of Calgary, Alberta, Canada

Abstract

Virtually all rodent neuroendocrine corticotropin-releasing-hormone (CRH) neurons are in the dorsal medial parvicellular (mpd) part of the paraventricular nucleus of the hypothalamus (PVH). They form the final common pathway for adrenocortical stress responses. Their activity is controlled by sets of GABA-, glutamate-, and catecholamine-containing inputs arranged in an interactive pre-motor network. Defining the nature and arrangement of these inputs can help clarify how stressor type and intensity information is conveyed to neuroendocrine neurons. Here we use immunohistochemistry with high-resolution 3-dimensional image analyses to examine the arrangement of single- and co-occurring GABA, glutamate, and catecholamine markers in synaptophysin-defined pre-synaptic terminals in the PVHmpd of unstressed rats and *Crh-IRES-Cre;Ai14* transgenic mice: respectively, vesicular glutamate transporter 2 (VGluT2), vesicular GABA transporter (VGAT), dopamine β-hydroxylase (DBH), and phenylethanolamine N-methyltransferase (PNMT). Just over half of all PVHmpd pre-synaptic terminals contain VGAT, with slightly less containing VGluT2. The vast majority of terminal appositions with mouse CRH neurons occur non-somatically. However, there are significantly more somatic VGAT than VGluT2 appositions. In the rat PVHmpd, about five times as many pre-synaptic terminals contain PNMT than DBH only. However, because epinephrine release has never been detected in the PVH, PNMT terminals may functionally be noradrenergic not adrenergic. PNMT and VGluT2 co-occur in some pre-synaptic terminals indicating the potential for co-transmission of glutamate and norepinephrine. Collectively, these results provide a structural basis for how GABA/glutamate/catecholamine interactions enable adrenocortical responses to fast-onset interosensory stimuli, and

Address for correspondence: Dr. Alan G. Watts, 3641 Watt Way, HNB 416, Los Angeles, CA 90089, Phone: 213-740-1497, Fax: 213-741-0561, watts@usc.edu.

CONFLICT OF INTEREST STATEMENT

All of the authors declare that they have no known or potential conflicts of interest.

ROLE OF THE AUTHORS

All authors had full access to all the data in the study and take responsibility for the integrity of the data and the accuracy of the data analysis. Study concept and design: CSJ, AGW. Acquisition of data: CSJ. Analysis and interpretation of data: CSJ, AGW. Drafting of the manuscript: CSJ, AGW. Critical revision of the manuscript for important intellectual content: CSJ, JSB, AGW. Statistical analysis: CSJ, AGW. Technical and material support: CSJ, AGW, JSB. Obtained funding: AGW, JSB.

more broadly, how combinations of PVH neurotransmitters and neuromodulators interact dynamically to control adrenocortical activity.

Graphical Abstract

The activity of neuroendocrine neurons in the paraventricular nucleus of the hypothalamus (PVH) is controlled by sets of pre-motor inputs. Using immunohistochemistry and confocal image analysis we examine single and co-occurrence of catecholaminergic, glutamatergic, and GABAergic markers in synaptophysin-defined axon terminals in the PVH region that mostly contains CRH neurons. We provide a structural basis for how these transmitter interactions enable adrenocortical responses to fast-onset interosensory stimuli, and more broadly, how combinations of PVH neurotransmitters and neuromodulators interact dynamically to control adrenocortical activity.

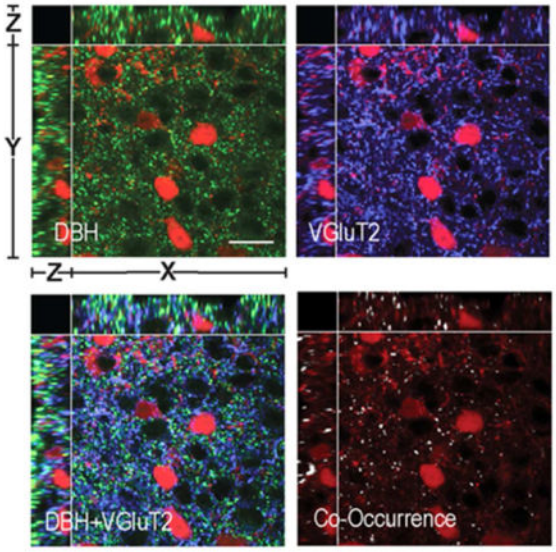

Keywords

Corticotropin-Releasing Hormone; Catecholamine; GABA; Glutamate; Synaptophysin; Pre-motor

INTRODUCTION

The medial parvicellular part, dorsal zone (mpd) of the rat and mouse paraventricular nucleus of the hypothalamus (PVH) mostly contains neuroendocrine motor neurons [Simmons and Swanson, 2009; Biag et al., 2012]. These neurons send axons to the median eminence where their terminals release various neurochemicals into the hypophysial portal vasculature to control hormone release from the anterior pituitary [Lechan et al., 1980; Wiegand & Price, 1980]. Of these, corticotropin-releasing hormone (CRH) neurons are perhaps the most well-studied, primarily because they form the apex of the hypothalamic-pituitary-adrenal (HPA) axis and control its response to all stressors, real or perceived.

CRH neurons are controlled by a complex pre-motor network that uses multiple transmitters and peptidergic modulators to relay information from various parts of the brain to the PVHmpd [Sawchenko and Swanson, 1983; Swanson and Sawchenko, 1983; Sawchenko et al., 1985; Herman and Cullinan, 1997; Herman et al., 2002, 2003; Watts, 2005; Bains et al., 2015]. Substantial evidence supports key roles for GABA and glutamate as primary controllers of neuroendocrine neurons [Boudaba et al., 1996, 1997; Herman et al., 2002; Herman et al., 2004; Kuzmiski et al., 2010; Inoue et al., 2013]. At least half of the pre-synaptic terminals in the medial hypothalamus are GABAergic [Decavel and van den Pol, 1992]. CRH neurons receive direct GABAergic synaptic innervation [Miklós and Kovács, 2002; Flak et al., 2009], and GABA-mediated inhibition is a crucial control element for these neurons [Cole and Sawchenko, 2002; Bali and Kovács, 2003; Wamsteeker and Bains, 2010; Bains et al., 2015]. Tonic activation of $GABA_A$ receptors inhibits neuroendocrine CRH activity, while blocking these receptors is sufficient to activate the HPA axis [Cole and Sawchenko, 2002]. In this way, neuroendocrine responses to stressors are dependent on GABA receptor mediated control of Cl^- homeostasis [Hewitt et al., 2009; Sarkar et al., 2011]. Similarly, numerous glutamate synapses are found within the PVH [Ziegler and Herman, 2000], and glutamate-containing pre-synaptic terminals appose CRH neurons [Wittmann et al., 2005]. Glutamatergic signaling activates the HPA axis [Ziegler and Herman, 2000; Bains et al., 2015].

A third set of inputs in the neuroendocrine pre-motor network are from hindbrain catecholamine neurons that innervate all subdivisions of the PVH [Swanson et al., 1981; Sawchenko and Swanson, 1982, 1983, Swanson and Sawchenko, 1983; Liposits et al., 1986b; Cunningham and Sawchenko, 1988; Cunningham et al., 1990]. They are defined by the presence or absence of three biosynthetic enzymes: tyrosine hydroxylase (TH), dopamine β-hydroxylase (DBH), and phenylethanolamine N-methyltransferase (PNMT) [Swanson et al., 1981]. PNMT-containing fibers predominate in the parvicellular PVH, with greatest innervation of the PVHmpd [Swanson et al., 1981; Cunningham et al., 1990], while the DBH-only innervation is mostly confined to the periventricular and magnocellular PVH [Swanson et al., 1981; Sawchenko and Swanson, 1982]. Catecholaminergic pre-synaptic terminals appose both magno- and parvicellular PVH neurons [Liposits et al., 1986a], including neuroendocrine CRH neurons [Liposits et al., 1986b].

Catecholaminergic afferents provide stimulus-specific information to the PVHmpd, particularly for acute physiological challenges [Ritter et al., 2011; Guyenet et al., 2013]. These neurons are indispensable for glucocorticoid responses to insulin-induced hypoglycemia, and are major contributors for responses to 2-deoxy-D-glucose (2DG) or GLP-1 agonists [Ritter et al., 2001, 2003; Khan et al., 2007; Lee et al., 2016]. They are also required to maintain the sensitivity of CRH mRNA to elevated levels of corticosterone [Kaminski and Watts, 2012] and to gate metaplasticity at GABA inputs on CRH neurons following an acute stress [Inoue et al, 2013]. However, they are not required for the daily rhythms of corticosterone secretion, or for neuroendocrine responses to psychogenic and other complex stressors [Ritter et al., 2003; Khan et al., 2011; Flak et al., 2014].

PVHmpd afferent systems are highly interactive [Herman et al., 2002, 2003; Watts & Sanchez-Watts, 2002; Watts, 2005; Yang et al., 2007, 2008; Wamsteeker and Bains, 2010;

Watts and Khan, 2013]. For example, catecholamine-mediated excitation of neurons within the PVH requires a glutamatergic component located in or around the PVH [Daftary et al., 2000; Herman et al., 2003]. Knowing this, some hindbrain catecholamine neurons contain vesicular glutamate transporter 2 (VGluT2) mRNA [Stornetta et al., 2002] raising the possibility that these neurons have an intrinsic glutamatergic transmitter component [El Mestikawy et al., 2011; DePuy et al., 2013]. It is also important to note that further afferent regulation derives from the many neuropeptides that co-occur in glutamatergic, GABAergic, and catecholaminergic inputs. These include NPY, AgRP, α-MSH, GLP-1, CART, PrRP, and PACAP. [Légrádi et al., 1998; Li et al., 2000; Matsumoto et al., 2000; Khan et al., 2013; Yoon et al., 2013; Zheng et al., 2015].

Our goal here is to elaborate how pre-synaptic terminals in the PVHmpd contribute to the functional anatomy of the pre-motor control network that controls neuroendocrine, and particularly CRH, neuronal activity [Herman et al., 2002, 2003; Watts, 2005; Watts and Khan, 2013]. To do this we analyze the distribution and neurochemical nature of synaptophysin-containing pre-synaptic terminals in the rat and mouse PVHmpd. Synaptophysin is a ubiquitous, vesicular membrane-bound protein [Wiedenmann et al., 1985] and its presence indicates pre-synaptic terminals [Masliah et al., 1990; Thiel, 1993; Flak et al., 2009; Kwon et al., 2011; Chavan et al., 2015]. Our analyses are limited to markers of glutamate (vesicular glutamate transporters 2 and 3; VGlut2, VGluT3) and GABA (vesicular GABA transporter; VGAT) neurotransmission, the catecholamines (PMNT and DBH), and neuropeptide Y (NPY) and agouti-related peptide (AgRP).

We used double- and triple-label immunohistochemistry (IHC) followed by high resolution three dimensional (3D) image analyses of confocal photomicrographs to determine three parameters: the relative abundance of different pre-synaptic terminal phenotypes within the PVHmpd of unstressed rats and mice; any co-occurrence of neurochemical markers within these terminals; and in mice, their appositions with CRH neurons.

MATERIALS AND METHODS

Animals

Nine adult male Sprague Dawley rats (~300g body weight) (Harlan) were housed two- or three-to-a-cage in a climate-controlled room (20–22°C), on a 12h light/dark cycle (lights on 0600h) with unrestricted access to food and water. Animals were acclimated and handled daily for at least five days before any procedures. The brains of six adult female *Crh-IRES-Cre;Ai14* mice [Wamsteeker-Cusulin et al., 2013] were shipped from the University of Calgary and immediately stored at −80°C until further processing. All procedures were approved by the local Institutional Care and Use Committees.

Perfusion and Sectioning

Rats were transcardially perfused with 100mL of cold 0.9% saline, followed by 500mL of cold 4% paraformaldehyde in a sodium borate solution (pH 9.5). Brains were removed and post-fixed overnight at 4°C in a solution of the same fixative, with the addition of 12% (w/v) sucrose. Brains were frozen in hexanes cooled by dry ice before being sectioned coronally at

20μm through the rostrocaudal extent of the PVH using a sliding microtome, then stored in a cryoprotectant solution (50% 0.05M sodium-phosphate buffer, 30% ethylene glycol, 20% glycerol) at −20°C until further processing. Seven series were reserved for IHC and one series was reserved for thionin staining to verify cytoarchitecture. Mouse brains were perfused and processed in the same manner but with a lower volume of fixative [Wamsteeker et al., 2010, 2013].

Immunohistochemistry

Sections were washed in tris-buffered saline (TBS, pH 7.4, six rinses for five minutes each at room temperature (RT)), and allowed to incubate for two hours (RT) in a blocking solution of TBS containing 2% (v/v) normal donkey serum (Chemicon, Temecula, CA, S30-100ML) and 0.03% (v/v) Triton X-100 (Sigma Aldrich, 9002-93-1). Sections were incubated in the same blocking solution containing various combinations of primary antibodies (Table 1) for 72 hours at 4°C. Sections were again washed in TBS and incubated in a solution of appropriate and corresponding species-sourced secondary antibodies (Table 2) overnight at 4°C. The sections were washed a final time as before then mounted onto Superfrost slides and allowed to air dry in the dark at RT. Once dry the slides were coverslipped with a solution of 50% TBS/50% glycerol, sealed with clear nail polish, and stored in the dark at 4°C.

The Characterization and Specificity of the Primary Antibodies

Rabbit anti-Agouti-Related Peptide (AgRP) antibody—Specificity was determined through preabsorption of the antiserum with the peptide antigen (Légrádi et al., 1999; Nilsson et al., 2008), following which the authors found no immunolabeling of AgRP in any sections. A single band between 14–21kDa was recognized by this antibody with western blot analysis of total duck brain or hypothalamic tissue extracts (Mirabella, Esposito, Squillacioti, De Luca, & Paino, 2004).

Mouse anti-Dopamine β Hydroxylase (DBH) monoclonal antibody—Western blot analysis recognizes a band of ~70kDa in rat tissue (Bruinstroop et al., 2012). Additionally, immunolabeling is abolished following preadsorption with the immunogen (Rinaman, 2001).

Rabbit anti-DBH antibody—This antibody was characterized using Western blot of purified DBH, and recognizes a triplet at approximately 72–74kDa. The manufacturers tested the antibody in the rat brainstem, cerebellum, and adrenal medulla. The antibody also replicates the known pattern of distribution when used simultaneously with another antibody against DBH (Halliday and McLachlan, 1991).

Sheep anti-Neuropeptide Y (NPY) antibody—Specificity was determined by the manufacturers through the use of radioimmunoassay, and immunolabeling was completely abolished following preabsorption with the immunogen. The antibody showed ~36% cross-reactivity with Peptide YY, though through the use of NPY knockout mice there is no immunolabeling by the antibody in either the forebrain or brainstem, indicating that there is no substantial cross-labeling with Peptide YY (Lee et al., 2013).

Rabbit anti-Phenylethanolamine N-Methyltransferase (PNMT) antibody—This antibody only labels the adrenergic cell groups (C1-3) of the hindbrain (Bohn et al., 1987; Rosin et al., 2006). Additional specificity controls were established through Western blot analysis, where the antibody was shown to recognize a single ~35kDa band, while labeling no bands from the liver, spleen, or cerebral cortex (Bohn et al., 1987).

Goat anti-Synaptophysin antibody—Specificity was verified by the manufacturers through Western blot analysis, where a single band was detected at ~38kDa in human, mouse, and rat brain tissue. Additionally, the generation of transgenic mice wherein the presumed presynaptic B-secretase enzyme is fused with yellow fluorescent protein showed colocalization with the synaptophysin antibody (Buggia-Prévot et al., 2014).

Rabbit anti-VGAT antibody—Western blot analysis show a single ~60kDa band in rat brain tissue (Chaudhry et al., 1998). Additionally, Western blot analyses of brain tissue from VGAT−/− knockout mice is completely devoid of this band (Martens et al., 2002).

Guinea pig anti-VGluT2 antibody—The manufacturer's Western blot analysis shows a single band at ~52kD. Additionally, when the tissue was incubated with the immunogen, immunolabeling was abolished (Bochorishvili et al., 2012).

Guinea pig anti-VGluT3 antibody—Western blot analysis recognizes a single ~65kDa band (from the manufacturers). Additionally, as reported by both the manufacturer and in the literature (Gabellec et al., 2007), preabsorption with the immunogen peptide abolishes all immunolabeling. Finally, specificity was further tested by the manufacturers on tissue from the rat central nervous system through the use of immunofluorescence histochemistry, where the staining pattern of the antibody was found to correspond with the known expression of VGluT3 mRNA in cell bodies (Fremeau et al., 2002; Gras et al., 2002; Soiza-Reilly and Commons, 2012).

Confocal Microscopy

Images were captured using a Zeiss 700 Laser Scanning Confocal Microscope equipped with a Zeiss AxioImager Z1 camera (Carl Zeiss MicroImaging, Inc., Thorwood, NY), using a 40x (numerical aperture 1.3) oil-corrected objective. An optical zoom of 1.6 was applied using the Zeiss Zen software (Zeiss Zen Black) to result in an image magnified to 64x. Images were taken using a unidirectional line scan at 1024 x 1024 pixels captured on an 8 bit gray scale. Each pixel was scanned twice and the result was averaged to reduce optical noise.

On this scale the intensity of a pixel is given a value ranging from 0 (black, no fluorescent labeling) to 255 (white, maximal fluorescent labeling). To ensure we captured the full range of fluorescent intensities, as well as to ensure proper alignment of each optical channel, images were first taken using fluorescent beads (15μm in diameter) (FocalCheck Fluorescence Microscope Test Slide #1, Invitrogen, F36909) expressing fluorophores for each laser line used. The lower limit (a black value of 0) was set by blocking the light path completely and verifying that all pixels registered a value of 0. This was adjusted using the *Offset* function in the Zeiss Zen software, and was done for each fluorophore channel used.

To set the upper limit, or saturated value of 255, we used the fluorescent beads. For each fluorophore channel the image was adjusted using the *Master Gain* function to ensure that all labeled pixels registered a value of 255, as the concentrated fluorescent dye in the beads is presumably more intense than labeling in physiological tissue. By ensuring that the camera is capable of capturing every possible value assigned to a pixel, we can analyze and compare different levels of fluorophore intensity.

The Airy unit was set to ~1.0 for all laser channels, allowing for an optimal signal to noise ratio based on the properties of each laser channel. Appropriate emission filters were applied to prevent bleed-through between optical channels. 3D images were constructed by taking images of planes (~1 μm) through the Z axis, with a frequency of ~0.4 μm, throughout the entire depth of the tissue section. Images were analyzed using Volocity software (PerkinElmer, version 6.3, Waltham, MA), operating on a MacBook Pro (Apple, Inc.).

The images for the rat PVHmpd were captured from sections corresponding to Levels 25–26 of the Swanson Rat Brain Atlas [Swanson, 2004]. Images of the mouse PVHmpd corresponded to Levels 61–62 of the Allen Reference Atlas [Dong, 2007; Biag et al., 2012]. Anatomical regions of interest were identified using adjacent Nissl-stained sections (Fig. 1).

Image Adjustments

A number of image corrections were employed before analysis. Images of the fluorescent beads were analyzed to ensure that all channels were properly aligned. At the scale of pre-synaptic terminals, any misalignment of images caused by light properties, external vibrations, or other sources of interference has serious consequences on accurate analysis. If all labeled fluorophores did not align in each dimension (X,Y, and Z), the alignment was corrected using the *Registration Correction* feature in Volocity. Subsequent experimental images were corrected using the same settings. To reduce optical aberrations caused by diffraction, particularly along the Z axis, image deconvolution was achieved through the *Iterative Restoration* feature using the *Measured Point Spread Function* in Volocity. One caveat to these methods is that our ability to resolve smaller appositions in the Z-axis is reduced compared to the X-Y axes because of spherical aberration. However, because our results are reported as relative comparisons and these differences are equally distributed across all samples, we believe they are adequately controlled.

Image Analysis

The Rat and Mouse PVH—Although the relative locations of the functional compartments of the rat and mouse PVH are comparable, the distribution of chemically defined neurons within them is somewhat more homogenous in the rat than the mouse [Simmons and Swanson, 2009; Biag et al., 2012]. In the rat most neuroendocrine CRH neurons are clustered in the PVHmpd between levels 25 and 26 [Swanson, 2004], where they are by far the most predominant peptide phenotype [Simmons and Swanson, 2009; Watts and Khan, 2013]. We therefore limited our analyses to these two levels of the rat PVHmpd (Fig. 1).

The distinct compartmental organization of the rat PVH is much less apparent in the mouse where the different chemical phenotypes are distributed more heterogeneously [Biag et al., 2012]. Most CRH neurons are located between levels 61–62 of the Allen mouse brain atlas [Dong, 2007]. To analyze these neurons in the mouse we used a transgenic line, *Crh-IRES-Cre;Ai14*, wherein all CRH neurons express the tdTomato fluorophore throughout their entirety [Wamsteeker et al., 2013] (Fig. 1). This endogenous labeling enables identification of pre-synaptic terminals that are immediately apposed to CRH neurons.

Fluorophore Colocalization—Dunn et al. [2011] have noted the importance of two components when assessing the colocalization of structures labeled with different fluorescent labels: co-occurrence, where two or more markers label the same physical structure; and correlation, wherein the fluorescent intensities of those co-occurring labels vary in a significantly correlated manner.

To determine the co-occurrence of two labels, the total number of each type of fluorescently-labeled structure was quantified within a defined region of interest in the PVHmpd. We then quantified those structures that were double- and/or triple-labeled, using Volocity software to build a protocol that identified each population of structures based on fluorophore expression. Thresholds were set to reduce aberrant signaling in both the volume and fluorescent-intensity parameters. To be considered a labeled structure a minimum volume threshold of 0.5 μm^3 was applied, along with a maximum threshold of 5μm^3 for pre-synaptic terminals. Thresholds for volume were determined through comparisons with previously published methods [Bouyer and Simerly, 2013]. Furthermore, a minimum threshold of two standard deviations above the mean background fluorescent intensity was applied. Soma were defined as appropriately-labeled structures with a volume $\geq$ 100 μm^3, but $\leq$ 500 μm^3 (mouse) and quantified through the Volocity software throughout the depth of the tissue. These values were determined to be the most appropriate thresholds to allow for the identification of single soma excluding axons and dendrites.

The *Intersect* function in Volocity was applied to determine the co-occurrence of overlapping populations, wherein structures containing both of the indicated fluorophores were counted as a separate population. To find those structures containing DBH but not PNMT the *Intersect* function was applied followed by the *Exclude Touching* function. This prohibited the quantification of DBH-labeled structures that also contained PNMT, leaving only single-labeled structures in the analysis.

To determine the locations of synaptophysin-labeled axon terminals that were apposed to CRH-positive structures in the mouse PVH we used the subtractive methods developed by Bouyer and Simerly [2013] adjusted to measure appositions per unit of surface area, rather than per unit of volume. We calculated the number appositions made to CRH soma by applying appropriate volume thresholds: >100 μm^3 for somatic regions; ≤99.9 μm^3 for non-somatic regions. We first determined the number of triple-labeled structures (synaptophysin/VGluT2 or VGAT/CRH) within the entire image. We then calculated appositions with non-somatic regions of CRH neurons by dividing the number of somatic appositions (ie. those made with td-Tom labeled structures) by the total number of appositions from the entire image for each terminal marker. The residual structures were designated non-somatic.

We were unable to identify DBH-immunoreactive (ir) appositions to non-somatic regions because of DBH and synaptophysin primary antibody species incompatibility. However, we used the voxel-to-voxel ('touching structures') approach described by Bouyer & Simerly [2013], to identify DBH-ir appositions with CRH neuronal soma.

Excel Analysis

Measurements from Volocity were transferred to Microsoft Excel for further analysis. The number of quantified structures (single-, double-, and triple-labeled) in each image was normalized to the total number of structures per 1000 μm^3, using the total measured volume of the tissue. Appositions were normalized to 100 μm^2 of measured CRH neuronal surface area. To determine the percent of co-occurrence of a single population with another population the total number of double-labeled structures was divided by the total number of single-labeled structures measured from each of the populations.

Validation Controls for the Methods of Assessing Co-Occurrence

We performed two sets of controls for the rat PVH to validate the co-occurrence methods.

1. *Theoretical Controls*. Sections containing the rat PVHmpd were co-labeled using two different antibodies against DBH: a mouse anti-DBH antibody and a rabbit anti-DBH antibody. Because these antibodies should theoretically identify the same structures, there should be no significant difference between the percent of mouse anti-DBH-labeled structures that express rabbit anti-DBH and the percent of rabbit anti-DBH-labeled structures that express mouse DBH.
2. *Technical Controls*. Sections containing the rat PVHmpd were co-labeled using a mouse anti-DBH antibody and a rabbit anti-PNMT antibody. The percent co-occurrence of the labeling with each antibody was determined. The organization of catecholamine biosynthetic pathways means that all structures containing PNMT must contain DBH, but not all DBH-labeled structures will contain PNMT [Swanson et al., 1981].

Statistics

Significant differences between group means were determined using Student's t test or a one-way analysis of variance (ANOVA) followed by Tukey's multiple comparison post hoc test, as appropriate (JMP Pro, version 12.1, SAS Institute Inc., Cary, NC). All data are expressed as the mean ± the standard error of the mean (S.E.M.). A p value of 0.05 or less was considered statistically significant for all tests.

RESULTS

Establishing the Validity of the Immunohistochemical and Quantitative Analyses

Theoretical Controls—Figure 2a)–d) shows structures in the rat PVHmpd labeled by the mouse or rabbit antibodies against DBH. We found that over 80% of the structures labeled by the mouse anti-DBH antibody were also labeled by the rabbit anti-DBH antibody (Fig. 2e). A similar percentage of the structures labeled by the rabbit anti-DBH antibody were also labeled by the mouse anti-DBH antibody (Fig. 2e). There was no statistical difference in

the percent of co-occurrence between these two measurements (Fig. 2e), indicating that the methods of calculating percent co-occurrence are theoretically valid.

Technical Controls—'Adrenergic' structures contain both DBH and PNMT, while 'noradrenergic' structures only contain DBH [Goldstein et al., 1972; Swanson et al., 1981]. When we double-labeled sections with DBH and PNMT antibodies (Fig. 2f–i) we found virtually all PNMT-labeled structures contain DBH (Fig. 2j), but significantly fewer DBH-labeled structures contain PNMT (Fig. 2j). These findings validate our ability to use these antibodies to differentiate between structures with these two different catecholaminergic phenotypes.

Vesicular Glutamate and GABA Transporter Distributions in the Rat PVH Region and their Organization within Terminal Appositions

Figure 3 shows the distribution of synaptophysin (Fig. 3a) VGluT2-ir (Fig. 3b), VGluT3-ir (Fig. 3c), and VGAT-ir (Fig. 3d) elements in the rat PVH. To determine if vesicular glutamate and GABA transporters were found only in pre-synaptic terminals in the rat and mouse PVHmpd, we assessed the percent co-occurrence of synaptophysin with VGluT2 or VGAT (Fig. 4).

Virtually every VGluT2-ir structure in the rat and mouse PVHmpd also contained synaptophysin (Figs. 4d,h). We also found that approximately half of all synaptophysin-ir terminals in the PVHmpd of both species contained VGluT2 (Fig. 4j). Only about one third of the VGluT3-ir structures in the rat PVHmpd co-occurred with synaptophysin, and about 10% of the synaptophysin co-occurred with VGluT3 (Fig. 4j), indicating that most VGluT3 is not situated in pre-synaptic terminals (Fig. 4j), which is consistent with previous findings [Seal and Edwards, 2006; Santos, 2009]. We also observed apparent VGlut3 in some axons and in the soma of some PVHpm magnocellular neurons (Fig. 3b), again consistent with the non-terminal expression of this transporter.

Like VGluT2, the vast majority of VGAT-ir co-occurred with synaptophysin in both rat and mouse PVHmpd (Fig. 4j) indicating that virtually all VGAT-ir structures are pre-synaptic terminals. Furthermore, over half of all synaptophysin-ir structures in the rat and mouse PVHmpd were also labeled for VGAT (Fig. 4j) indicating substantial GABAergic innervation in both species.

VGluT2 and VGAT Co-Occur in a Population of Terminals in the PVHmpd

When we analyzed the co-occurrence of VGluT2 and VGAT in the rat PVHmpd (Fig. 5) we found approximately 8% of synaptophysin-labeled pre-synaptic terminals contained both vesicular transporters (Fig. 5e). The number of these double-labeled pre-synaptic terminals was considerably less than the pre-synaptic terminals single-labeled for either VGluT2 or VGAT only (Fig. 5e). VGluT2 and VGAT co-occurrence could not be assessed in the mouse because of species incompatibility with the appropriate antibodies.

Catecholaminergic Innervation Patterns in the Rat PVH

DBH (Fig. 6a) and PNMT (Fig. 6b) are differentially distributed in the rat PVH. PNMT was most abundant in the PVHmpd (Fig. 6c, yellow only), while DBH only (Fig. 6c, blue only) was most concentrated in the PVHpm and PVHmpv. The remaining compartments (PVHdp and PVHpv) contained a mixture of PNMT and DBH only. When we analyzed the number of terminals containing synaptophysin and either DBH-only or PNMT in the PVHmpd we found four times more PMNT than DBH-only terminals (Fig. 6d), which is consistent with previous reports showing that PNMT-containing afferents preferentially innervate the parvicellular parts of the PVH that mediate neuroendocrine responses [Swanson et al., 1981; Cunningham et al., 1990].

Catecholaminergic Axon Terminals Express VGluT2 in the PVHmpd of the Rat and the Mouse

In the rat PVHmpd, approximately 25% of all VGluT2-containing pre-synaptic terminals also expressed catecholaminergic markers (Fig. 7a–d, e–h). However, Figure 7i) shows that there was a much higher incidence of VGluT2 co-occurrence in PNMT-containing (21%) than in DBH-only-containing terminals (4%).

We also analyzed the number of pre-synaptic terminals and the co-occurrence of VGluT2 and DBH in the mouse (Fig. 7j–m). Because the PNMT antibody did not produce specific staining in mouse brain sections, we were unable to differentiate PNMT-ir structures from DBH-only-ir structures. Like the rat PVHmpd, there were significantly more VGluT2-containing pre-synaptic terminals than catecholaminergic pre-synaptic terminals in the female mouse PVHmpd (Fig. 7n). VGluT2 and DBH co-occur in the mouse, but there are significantly fewer double-labeled pre-synaptic terminals than either VGluT2-only or catecholaminergic-only pre-synaptic terminals (Fig. 7n).

Catecholamines and NPY Co-Occur in Axon Terminals in the PVHmpd of the Rat

Figure 8 shows that almost two thirds of the NPY-ir structures co-occur with either DBH or PNMT or both, while the remaining third co-occurs with AgRP. Furthermore, almost all of the structures labeled with AgRP also contained NPY.

Appositions to CRH Neurons in the Mouse PVHmpd

There were large numbers of synaptophysin-labeled axon terminal in the mouse PVHmpd (Fig. 9a–c,m). We found approximately twice the number of somatic VGAT-containing appositions (Fig. 9d–f,n) than either VGluT2- (Fig. 9g–i,n) or DBH-containing (Fig. 9j–l,n) appositions.

We found that approximately 90% of synaptophysin-, VGluT2-, and VGAT-containing appositions were with non-somatic regions rather than somatic regions (Fig. 9o). Although we could not account for the cellular locations of all non-somatic appositions, many VGAT terminals were clearly apposed to what appeared to be dendrites of CRH neurons (Fig. 10).

DISCUSSION

Our goal was to determine the configuration and the degree of co-occurrence of protein markers for glutamate-, GABA-, and catecholamine-containing presynaptic terminals in the rat and mouse PVHmpd. Five main findings are evident (Fig. 11). First, there are somewhat more VGAT- (GABAergic) than VGluT2-containing (glutamatergic) pre-synaptic terminals. Second, about 80% of catecholamine pre-synaptic terminals contain PNMT, the remainder are DBH-only. Third, almost 20% of all VGluT2-containing (glutamatergic) terminals also contain PNMT/DBH or DBH-only, with VGluT2 being five times more prevalent in PNMT- than DBH-only-containing terminals. Fourth, while there are substantially more terminal appositions of all types to non-somatic regions of mouse CRH neurons, there are significantly more somatic GABAergic appositions than either glutamatergic or catecholaminergic appositions. Finally, our results are consistent with the finding that approximately two-thirds of the NPY innervation to neuroendocrine CRH neurons originates from the catecholaminergic cell groups of the hindbrain [Bai et al., 1985; Sawchenko et al., 1985; Füzesi et al., 2007], with the remainder originating from other sources, for example the arcuate and dorsomedial nuclei of the hypothalamus [Bai et al., 1985; Füzesi et al., 2007; Lee et al., 2013]. The NPY innervation originating from the arcuate nucleus also contains AgRP [Hahn et al., 1998] and is GABAergic [Tong et al., 2008].

Glutamate/GABA

Figure 11 shows that presynaptic terminals containing VGluT2 and VGAT account for at least 85% of the total number of synaptophysin-labeled terminals in the rat and mouse PVHmpd. Of these, just over half contain VGAT. These numbers agree with previous electron microscopic (EM) surveys of GABAergic synapses [Decavel and van den Pol, 1990; Miklós and Kovács, 2003, 2011].

GABAergic terminals make direct contact with CRH neurons and use $GABA_A$ receptor signaling to exert strong inhibitory influence over them and the HPA axis [Cole and Sawchenko, 2002; Miklós and Kovács, 2002, 2011; Bali and Kovács, 2003; Cullinan, 2000; Cullinan et al., 2008]. We found twice as many VGAT-containing terminals apposed to CRH neuronal soma than VGluT2- or DBH-containing terminals to help enable this strong inhibitory control.

The second largest group of synaptophysin-labeled terminals contain VGluT2 (Fig. 11). The fact that afferent activation elicits glutamatergic excitatory post-synaptic potentials in parvicellular PVH neurons [Wuarin and Dudek, 1991; Daftary et al., 2000], is consistent with the likelihood that VGluT2 expressed in PVHmpd terminals is associated with pre-synaptic glutamate release [Bellocchio et al., 1998]. The lack of suitable markers has made EM examinations of glutamatergic synapses in the PVHmpd more challenging than for GABA, but the consensus is that glutamate provides a significant innervation to the PVH including CRH neurons [van den Pol et al., 1990; Wittmann et al., 2005]. Our results are consistent with these findings.

To understand how afferent networks control neuroendocrine neurons it is important to know on which parts of these neurons particular inputs form synapses. Electron microscopy (EM)

provides the most detailed level of analysis. These EM studies consistently indicate that the great majority of PVH pre-synaptic terminals are found on dendrites [Decavel and van den Pol, 1990]. Using a CRH reporter mouse [Wamsteeker et al., 2013] we found only about 10% of all synaptophysin-defined terminals apposed to CRH neuronal soma. These findings are consistent with previous EM distribution analyses of somatic versus non-somatic synapses in the rat medial parvicellular PVH [Decavel and van den Pol, 1990; Miklós and Kovács, 2011]. Our percentages are somewhat higher than those reported by Miklós and Kovács (72%) [2011] perhaps because they used colchicine to help visualize CRH neurons. Colchicine can dramatically alter CRH neuronal morphology, including somatic area, and dendritic spine number and density [Rho and Swanson, 1989]. We found that somatically located GABAergic terminals are significantly more abundant than glutamatergic and DBH-containing terminals. The remaining synaptophysin-defined terminals are most likely axo-dendritic, but with no apparent differences between the proportions of GABAergic and glutamatergic terminals. These results are again consistent with GABAergic inhibition being the predominant control component for these neurons.

Although we found some VGluT3/synaptophysin co-occurrence that may correspond to synaptic glutamate release, it was much less frequent than with VGluT2 or VGAT, meaning that VGluT3 has a more widespread non-terminal distribution within PVHmpd neurons than the other two transporters. The apparent expression of VGluT3 in the soma of magnocellular neurons is consistent with this view. VGluT3 is found in pre-synaptic terminals, cell bodies, and dendrites of neurons not traditionally considered glutamatergic, particularly serotonergic and cholinergic neurons [Fremeau et al., 2002; Gras et al., 2002; Herzog et al., 2004; Kljakic et al., 2017; Somogyi et al., 2004; Commons, 2009]. Therefore VGluT3/synaptophysin co-occurrence may be in serotonergic or possibly cholinergic terminals rather than glutamatergic (Fig. 11).

VGluT2 and VGAT Co-occurrence

We found a relatively small number of pre-synaptic terminals containing both VGluT2 and VGAT. Although these populations have generally been considered mutually exclusive it is evident that this is not always the case [Boudaba et al., 1996; Ottem et al., 2004; Zander et al., 2010]. While the primary function of vesicular transporters is to package fast-acting neurotransmitters into synaptic vesicles [McIntire et al., 1997; Chaudhry et al., 1998; Fremeau et al., 2002; Herzog et al., 2001], the presence of the VGluTs does not unambiguously mark synaptically releasable glutamate. When VGluTs are found in the same terminals as other transporters, including VGAT, they can augment the packaging ability of the principal transmitter transporter, a process called vesicular synergy [El Mestikawy et al., 2011; Münster-Wandowski et al., 2016]. Additionally, VGluTs may be involved in the transport of inorganic phosphate into vesicles, independent of glutamate transport [Ni et al., 1994; Aihara et al., 2000; Juge et al., 2006]. Collectively these results mean that PVHmpd pre-synaptic terminals with VGluT2/VGAT co-occurrence are more likely GABAergic than glutamatergic (Fig. 11).

Catecholamines

The locations of catecholaminergic neurons have traditionally been defined by the expression of their biosynthetic enzymes: dopaminergic (A9 etc. groups; TH, but not DBH or PNMT); noradrenergic (A1–A8 groups; TH and DBH, but not PNMT); and adrenergic (C1– C3 groups; all three enzymes). Using this nomenclature, virtually all the catecholaminergic innervation of the PVH originates from two medullary locations: the ventrolateral medulla (VLM) (A1, A1/C1, and C1) and the nucleus of the solitary tract (NTS) (A2 and C2), although some periventricular noradrenergic inputs come from the locus coeruleus (A6) [Cunningham and Sawchenko, 1988]. The A1 group primarily innervates magnocellular neurons; the A2 group innervates both parvi- and magnocellular parts [Swanson et al., 1981; Cunningham and Sawchenko, 1988]; while the C1 and C2 groups target its parvicellular parts [Swanson et al., 1981; Cunningham et al., 1990].

VGluT2 mRNA is found in the majority of PNMT-expressing cell groups, as well as in some A2 neurons, but its expression appears to be most widespread in C1 neurons [Stornetta et al., 2002]. Guyenet and colleagues have provided compelling evidence that glutamate is the primary ionotropic transmitter in those C1 neurons that project to the spinal cord and hindbrain to control cardiovascular processes [DePuy et al., 2013].

C1 neurons that project to the hypothalamus are found at somewhat different locations in the VLM from those with hindbrain or spinal cord projections [Tucker et al., 1987; Guyenet et al., 2013]. These C1 neurons project heavily to the PVHmpd [Swanson et al., 1981; Cunningham et al., 1990]. They make asymmetric synapses with their targets [Liposits et al., 1986ab], which are structurally similar to the glutamatergic synapses made by C1 neurons in the hindbrain [Sheng and Kim, 2011; DePuy et al., 2013]. We now provide the first evidence that a significant number of DBH/PNMT-containing axon terminals in the PVHmpd also contain VGluT2, meaning that—like caudally directed C1 neurons—glutamate is probably their primary ionotropic transmitter. Previous reports suggest that catecholaminergic neurons engage glutamatergic interneurons to alter parvicellular neuronal function in the PVH [Daftary et al., 2000; Herman et al., 2003], but our results now indicate that at least a subset of these catecholaminergic inputs can themselves release glutamate.

Are catecholamines released by the terminals of C1 or C2 neurons projecting into the PVH? There is a notable lack of direct evidence for epinephrine and/or norepinephrine release from the axon terminals, dendrites, or other parts of caudally projecting C1 neurons [Guyenet et al., 2013]. The fact that PNMT in the hindbrain and spinal cord does not reliably indicate the presence of releasable epinephrine is consistent with this view [Sved, 1989]. These neurons synthesize but do not store epinephrine in vesicles, most likely because elevated levels of monoamine oxidase quickly degrades non-vesicular epinephrine [Sved, 1989; 1990]. We find approximately five times as many PNMT-containing pre-synaptic terminals in the PVHmpd as those containing only DBH. Conventionally this should mean that these neurons will release epinephrine and norepinephrine, respectively. Therefore, it is very surprising that epinephrine release in the PVH has never been detected by microdialysis or fast-scan cyclic voltammetry after various challenges [Pacak et al., 1995,1999,2001; Gerth and Roitman, 2016]. The difference between C1 neurons projecting to the hindbrain/spinal cord and those that project to the hypothalamus may result from how hypothalamic monoamine

oxidase acts on epinephrine and norepinephrine, the different cellular locations of DBH (vesicular) and PNMT (cytoplasmic) [Sved, 1990], and the reported absence of a membrane transporter in most C1 neurons [Lorang et al., 1994; Comer et al., 1998].

A lack of measureable epinephrine release in the PVH has two interpretational consequences. First, DBH- and PNMT-containing terminals in the PVH both release norepinephrine, and therefore both should be considered noradrenergic (Fig. 11). Second, the presence or absence of PNMT may not coincide with different releasable catecholamines. Instead it identifies two anatomically distinct neuronal populations with different neuropeptides, afferents, and functional consequences for post-synaptic PVH neurons. For example, PNMT-containing neurons are preferentially recruited by 2DG-induced glucoprivation [Ritter et al., 1998], and particularly by insulin-induced hypoglycemia, which activates more neurons in the C1 region than in A1, A2, and C2 [Jokiaho et al., 2014].

The post-synaptic effects of norepinephrine on PVH parvicellular neurons are varied and complex. Applying norepinephrine to hypothalamic slices containing the PVH increases the firing rates of most parvicellular neurons using ionotropic glutamate receptor-, α1 adrenoreceptor-, and mitogen-activated protein kinase kinase (MEK)-dependent mechanisms [Daftary et al., 2000; Khan et al., 2011]. Conversely, a minority of neurons are inhibited by norepinephrine using β-adrenoreceptor-dependent mechanism [Daftary et al., 2000]. Our structural results now show that at least part of the glutamatergic component in this effect likely originates directly from mostly C1-originating and PNMT-containing terminals in the PVHmpd.

While the relationship between the mechanisms used by norepinephrine to alter parvicellular neuron excitation and the various neuronal components in the PVHmpd are unknown, one key synaptic mechanism is worth noting. Norepinephrine can regulate GABA synaptic plasticity using a mGluR1-dependent metaplastic effect on the ability of GABA synapses to express LTP [Inoue et al., 2013]. This occurs because the norepinephrine released by a stressor into the PVHmpd increases post-synaptic $GABA_A$ receptor membrane insertion, thereby increasing GABA LTP, and consequently post-synaptic responsiveness to subsequent stressors [Bains et al., 2015].

Conclusions

Our results reveal complex relationships between glutamate, GABA, and norepinephrine in pre-synaptic terminals of the neuroendocrine pre-motor networks in the PVHmpd. Complexity is further increased when we consider the other co-occurring peptides and other signaling systems that are known to be present in PVHmpd afferents. An important functional consideration is that the inability of other studies to detect epinephrine release in the PVH suggests that all catecholamine terminals in the PVHmpd, including those containing PNMT, release norepinephrine. For CRH neurons, the dynamic regulation of their pre-synaptic signaling molecules should significantly increase synaptic flexibility in a way that is well-placed to mediate adaptive CRH neuronal responses to different glucocorticoid environments and stressor exposures [Watts, 2005]. Further investigation is needed to determine how and when this dynamic regulation is mediated—including for

example, whether the various signaling molecules are arranged in a co-release or a co-transmission configuration [Vaaga et al., 2014]—and under what circumstances the various signals are released.

Acknowledgments

Funding: This work was funded by grants from the National Institutes of Health (R01 NS029728 to AGW) and the Canadian Institutes of Health Research (MOP 86501 to JSB)

LITERATURE CITED

Abbott SB, Kanbar R, Bochorishvili G, Coates MB, Stornetta RL, Guyenet PG. C1 neurons excite locus coeruleus and A5 noradrenergic neurons along with sympathetic outflow in rats. Journal of Physiology. 2012; 590(12):2897–2915. DOI: 10.1113/jphysiol.2012.232157 [PubMed: 22526887]

Aihara Y, Mashima H, Onda H, Hisano S, Kasuya H, Hori T, Yamada S, Tomura H, Yamada Y, Inoue I, Kojima I. Molecular Cloning of a Novel Brain-Type Na+-Dependent Inorganic Phosphate Cotransporter. Journal of Neurochemistry. 2000; 74(6):2622–2625. [PubMed: 10820226]

Bai FL, Yamano M, Shiotani Y, Emson PC, Smith AD, Powell JF, Tohyama M. An arcuato-paraventricular and -dorsomedial hypothalamic neuropeptide Y-containing system which lacks noradrenaline in the rat. Brain Research. 1985; 331(1):172–175. [PubMed: 2859091]

Bains JS, Wamsteeker Cusulin JI, Inoue W. Stress-related synaptic plasticity in the hypothalamus. Nature Reviews Neuroscience. 2015; 16:377–88. DOI: 10.1038/nrn3881 [PubMed: 26087679]

Bali B, Kovács KJ. GABAergic control of neuropeptide gene expression in parvocellular neurons of the hypothalamic paraventricular nucleus. European Journal of Neuroscience. 2003; 18(6):1518–1526. [PubMed: 14511331]

Bellocchio EE, Hu H, Pohorille A, Chan J, Pickel VM, Edwards RH. The localization of the brain-specific inorganic phosphate transporter suggests a specific presynaptic role in glutamatergic transmission. Journal of Neuroscience. 1998; 18(21):8648–8659. [PubMed: 9786972]

Biag J, Huang Y, Gou L, Hintiryan H, Askarinam A, Hahn JD, Toga AW, Dong HW. Cyto- and chemoarchitecture of the hypothalamic paraventricular nucleus in the C57BL/6J male mouse: A study of immunostaining and multiple fluorescent tract tracing. Journal of Comparative Neurology. 2011; 520(1):6–33. DOI: 10.1002/cne.22698

Bochorishvili G, Stornetta RL, Coates MB, Guyenet PG. Pre- Bötzinger complex receives glutamatergic innervation from galaninergic and other retrotrapezoid nucleus neurons. Journal of Comparative Neurology. 2012; 520(5):1047–1061. DOI: 10.1002/cne.22769 [PubMed: 21935944]

Bohn MC, Dreyfus CF, Friedman WJ, Markey KA. Glucocorticoid effects on phenylethanolamine N-methyltransferase (PNMT) in explants of embryonic rat medulla oblongata. Brain Research. 1987; 465(1–2):257–266. [PubMed: 3440206]

Boudaba C, Szabo K, Tasker JG. Physiological mapping of local inhibitory inputs to the hypothalamic paraventricular nucleus. Journal of Neuroscience. 1996; 16(22):7151–7160. [PubMed: 8929424]

Bouyer K, Simerly RB. Neonatal leptin exposure specifies innervation of presympathetic hypothalamic neurons and improves the metabolic status of leptin-deficient mice. Journal of Neuroscience. 2013; 33(2):840–851. DOI: 10.1523/JNEUROSCI.3215-12.2013 [PubMed: 23303959]

Bruinstroop E, Cano G, Vanderhorst VG, Cavalcante JC, Wirth J, Sena-Esteves M, Saper CB. Spinal projections of the A5, A6 (locus coeruleus), and A7 noradrenergic cell groups in rats. Journal of Comparative Neurology. 2012; 520(9):1985–2001. DOI: 10.1002/cne.23024 [PubMed: 22173709]

Buggia-Prévot V, Fernandez CG, Riordan S, Vetrivel KS, Roseman J, Waters J, Bindokas VP, Vassar R, Thinakaran G. Axonal BACE1 dynamics and targeting in hippocampal neurons: a role for Rab11 GTPase. Molecular neurodegeneration. 2014; 9(1):1.doi: 10.1186/1750-1326-9-1 [PubMed: 24386896]

Chaudhry FA, Reimer RJ, Bellocchio EE, Danbolt NC, Osen KK, Edwards RH, Storm-Mathisen J. The vesicular GABA transporter, VGAT, localizes to synaptic vesicles in sets of glycinergic as well as GABAergic neurons. Journal of Neuroscience. 1998; 18(23):9733–9750. [PubMed: 9822734]

Chavan V, Willis J, Walker SK, Clark HR, Liu X, Fox MA, Srivastava S, Mukherjee K. Central presynaptic terminals are enriched in ATP but the majority lack mitochondria. PloS One. 2015; 10(4):e0125185.doi: 10.1371/journal.pone.0181140 [PubMed: 25928229]

Cole RL, Sawchenko PE. Neurotransmitter regulation of cellular activation and neuropeptide gene expression in the paraventricular nucleus of the hypothalamus. Journal of Neuroscience. 2002; 22(3):959–969. [PubMed: 11826124]

Comer AM, Qi J, Christie DL, Gibbons HM, Lipski J. Noradrenaline transporter expression in the pons and medulla oblongata of the rat: localisation to noradrenergic and some C1 adrenergic neurones. Molecular Brain Research. 1998; 62(1):65–76. [PubMed: 9795140]

Commons KG. Locally collateralizing glutamate neurons in the dorsal raphe nucleus responsive to substance P contain vesicular glutamate transporter 3 (VGLUT3). Journal of Chemical Neuroanatomy. 2009; 38(4):273–281. DOI: 10.1016/j.jchemneu.2009.05.005 [PubMed: 19467322]

Cullinan WE. GABA(A) receptor subunit expression within hypophysiotropic CRH neurons: a dual hybridization histochemical study. Journal of Comparative Neurology. 2000; 419(3):344–351. [PubMed: 10723009]

Cullinan WE, Ziegler DR, Herman JP. Functional role of local GABAergic influences on the HPA axis. Brain Structure and Function. 2008; 213(1–2):63–72. DOI: 10.1007/s00429-008-0192-2 [PubMed: 18696110]

Cunningham ET Jr, Sawchenko PE. Anatomical specificity of noradrenergic inputs to the paraventricular and supraoptic nuclei of the rat hypothalamus. Journal of Comparative Neurology. 1988; 274(1):60–76. [PubMed: 2458397]

Cunningham ET Jr, Bohn MC, Sawchenko PE. Organization of adrenergic inputs to the paraventricular and supraoptic nuclei of the hypothalamus in the rat. Journal of Comparative Neurology. 1990; 292(4):651–667. [PubMed: 2324319]

Daftary SS, Boudaba, Tasker JG. Noradrenergic Regulation of Parvocellular Neurons in the Rat Hypothalamic Paraventricular Nucleus. Neuroscience. 2000; 96(4):743–751. [PubMed: 10727792]

Decavel C, van den Pol AN. GABA: a dominant neurotransmitter in the hypothalamus. Journal of Comparative Neurology. 1990; 302(4):1019–1037. [PubMed: 2081813]

Decavel C, van den Pol AN. Converging GABA- and glutamate-immunoreactive axons make synaptic contact with identified hypothalamic neurosecretory neurons. Journal of Comparative Neurology. 1992; 316(1):104–16. [PubMed: 1349310]

DePuy SD, Stornetta RL, Bochorishvili G, Deisseroth K, Witten I, Coates M, Guyenet PG. Glutamatergic neurotransmission between the C1 neurons and the parasympathetic preganglionic neurons of the dorsal motor nucleus of the vagus. Journal of Neuroscience. 2013; 33(4):1486–1497. DOI: 10.1523/JNEUROSCI.4269-12.2013 [PubMed: 23345223]

Dong, HW. The Allen reference atlas: A digital color brain atlas of the C57Bl/6J male mouse. John Wiley & Sons Inc; 2007. (Online at: http://mouse.brain-map.org/static/atlas)

Dunn KW, Kamocka MM, McDonald JH. A practical guide to evaluating colocalization in biological microscopy. American Journal of Physiology, Cell Physiology. 2011; 300(4):C723–742. DOI: 10.1152/ajpcell.00462.2010 [PubMed: 21209361]

El Mestikawy S, Wallén-Mackenzie Å, Fortin GM, Descarries L, Trudeau LE. From glutamate co-release to vesicular synergy: vesicular glutamate transporters. Nature Reviews Neuroscience. 2011; 12(4):204–216. DOI: 10.1038/nrn2969 [PubMed: 21415847]

Flak JN, Myers B, Solomon MB, McKlveen JM, Krause EG, Herman JP. Role of paraventricular nucleus-projecting norepinephrine/epinephrine neurons in acute and chronic stress. European Journal of Neuroscience. 2014; 39(11):1903–1911. [PubMed: 24766138]

Flak JN, Ostrander MM, Tasker JG, Herman JP. Chronic stress-induced neurotransmitter plasticity in the PVH. Journal of Comparative Neurology. 2009; 51(2):156–165. DOI: 10.1111/ejn.12587

Fremeau RT Jr, Burman J, Qureshi T, Tran CH, Proctor J, Johnson J, Zhang H, Sulzer D, Copenhagen DR, Storm-Mathisen J, Reimer RJ, Chaudhry FA, Edwards RH. The identification of vesicular glutamate transporter 3 suggests novel modes of signaling by glutamate. Proceedings of the National Academy of Science, USA. 2002; 99(22):14488–14493. DOI: 10.1073/pnas.222546799

Füzesi T, Wittmann G, Liposits Z, Lechan RM, Fekete C. Contribution of noradrenergic and adrenergic cell groups of the brainstem and agouti-related protein-synthesizing neurons of the arcuate nucleus to neuropeptide-y innervation of corticotropin-releasing hormone neurons in hypothalamic paraventricular nucleus of the rat. Endocrinology. 2007; 148(11):5442–5450. DOI: 10.1210/en.2007-0732 [PubMed: 17690163]

Gabellec MM, Panzanelli P, Sassoe-Pognetto M, Lledo PM. Synapse- specific localization of vesicular glutamate transporters in the rat olfactory bulb. European Journal of Neuroscience. 2007; 25(5): 1373–1383. DOI: 10.1111/j.1460-9568.2007.05400.x [PubMed: 17425564]

Gerth, AI., Roitman, MF. Program No. 731.06. 2016 Neuroscience Meeting Planner. San Diego, CA: Society for Neuroscience; 2016. Electrical stimulation of the ventral noradrenergic bundle results in frequency dependent norepinephrine release in the paraventricular nucleus of the hypothalamus. Online

Goldstein M, Fuxe K, Hökfelt T. Characterization and tissue localization of catecholamine synthesizing enzymes. Pharmacological Reviews. 1972; 24(2):293–309. [PubMed: 4564603]

Gras C, Herzog E, Bellenchi GC, Bernard V, Ravassard P, Pohl M, Gasnier B, Giros B, El Mestikawy S. A third vesicular glutamate transporter expressed by cholinergic and serotoninergic neurons. Journal of Neuroscience. 2002; 22(13):5442–5451. [PubMed: 12097496]

Guyenet PG, Stornetta RL, Bochorishvili G, Depuy SD, Burke PG, Abbott SB. C1 neurons: the body's EMTs. American Journal of Physiology, Regulatory, Integrative and Comparative Physiology. 2013; 305(3):R187–204. DOI: 10.1152/ajpregu.00054.2013

Halliday GM, McLachlan EM. A comparative analysis of neurons containing catecholamine-synthesizing enzymes and neuropeptide Y in the ventrolateral medulla of rats, guinea-pigs and cats. Neuroscience. 1991; 43(2–3):531–550. [PubMed: 1681467]

Hahn TM, Breininger JF, Baskin DG, Schwartz MW. Coexpression of Agrp and NPY in fasting-activated hypothalamic neurons. Nature Neuroscience. 1998; 1(4):271–272. [PubMed: 10195157]

Herman JP, Cullinan WE. Neurocircuitry of stress: central control of the hypothalamo–pituitary–adrenocortical axis. Trends in Neuroscience. 1997; 20(2):78–84.

Herman JP, Tasker JG, Ziegler DR, Cullinan WE. Local circuit regulation of paraventricular nucleus stress integration: glutamate–GABA connections. Pharmacology, Biochemistry, and Behavior. 2002; 7(3):457–468.

Herman JP, Figueiredo H, Mueller NK, Ulrich-Lai Y, Ostrander MM, Choi DC, Cullinan WE. Central mechanisms of stress integration: hierarchical circuitry controlling hypothalamo–pituitary–adrenocortical responsiveness. Frontiers in Neuroendocrinology. 2003; 24(3):151–180. [PubMed: 14596810]

Herzog E, Bellenchi GC, Gras C, Bernard V, Ravassard P, Bedet C, Gasnier B, Giros B, El Mestikawy S. The existence of a second vesicular glutamate transporter specifies subpopulations of glutamatergic neurons. Journal of Neuroscience. 2001; 21(22):RC181. [PubMed: 11698619]

Herzog E, Gilchrist J, Gras C, Muzerelle A, Ravassard P, Giros B, Gaspar P, El Mestikawy. Localization of VGLUT3, the vesicular glutamate transporter type 3, in the rat brain. Neuroscience. 2004; 123(4):983–1002. [PubMed: 14751290]

Hewitt SA, Wamsteeker JI, Kurz EU, Bains JS. Altered chloride homeostasis removes synaptic inhibitory constraint of the stress axis. Nature Neuroscience. 2009; 12:438–43. DOI: 10.1038/nn.2274 [PubMed: 19252497]

Inoue W, Baimoukhametova DV, Füzesi T, Wamsteeker Cusulin JI, Koblinger K, Whelan PJ, Pittman QJ, Bains JS. Noradrenaline is a stress-associated metaplastic signal at GABA synapses. Nature Neuroscience. 2013; 16(5):605–612. DOI: 10.1038/nn.3373 [PubMed: 23563580]

Jokiaho AJ, Donovan CM, Watts AG. The rate of fall of blood glucose determines the necessity of forebrain-projecting catecholaminergic neurons for male rat sympathoadrenal responses. Diabetes. 2014; 63(8):2854–2865. DOI: 10.2337/db13-1753 [PubMed: 24740574]

Juge N, Yoshida Y, Yatsushiro S, Omote H, Moriyama Y. Vesicular glutamate transporter contains two independent transport machineries. Journal of Biological Chemistry. 2006; 281(51):39499–39506. DOI: 10.1074/jbc.M607670200 [PubMed: 17046815]

Kaminski KL, Watts AG. Intact catecholamine inputs to the forebrain are required for appropriate regulation of corticotrophin-releasing hormone and vasopressin gene expression by corticosterone

in the rat paraventricular nucleus. Journal of Neuroendocrinology. 2012; 24(12):1517–1526. DOI: 10.1111/j.1365-2826.2012.02363.x [PubMed: 22831701]

Khan AM, Ponzio TA, Sanchez-Watts G, Stanley BG, Hatton GI, Watts AG. Catecholaminergic control of mitogen-activated protein kinase signaling in paraventricular neuroendocrine neurons in vivo and in vitro: a proposed role during glycemic challenges. Journal of Neuroscience. 2007; 27(27):7344–7360. DOI: 10.1523/JNEUROSCI.0873-07.2007 [PubMed: 17611287]

Khan AM, Kaminski KL, Sanchez-Watts G, Ponzio TA, Kuzmiski JB, Bains JS, Watts AG. MAP kinases couple hindbrain-derived catecholamine signals to hypothalamic adrenocortical control mechanisms during glycemia-related challenges. Journal of Neuroscience. 2011; 31(50):18479–18491. DOI: 10.1523/JNEUROSCI.4785-11.2011 [PubMed: 22171049]

Khan AM, Walker EM, Dominguez N, Watts AG. Neural input is critical for arcuate hypothalamic neurons to mount intracellular signaling responses to systemic insulin and deoxyglucose challenges in male rats: implications for communication within feeding and metabolic control networks. Endocrinology. 2013; 155(2):405–416. DOI: 10.1210/en.2013-1480 [PubMed: 24265445]

Kljakic O, Janickova H, Prado VF, Prado MAM. Cholinergic/glutamatergic co-transmission in striatal cholinergic interneurons: new mechanisms regulating striatal computation. Journal of Neurochemistry. 2017; 142(Suppl 2):90–102. DOI: 10.1111/jnc.14003 [PubMed: 28421605]

Kwon SE, Chapman ER. Synaptophysin regulates the kinetics of synaptic vesicle endocytosis in central neurons. Neuron. 2011; 70(5):847–854. DOI: 10.1016/j.neuron.2011.04.001 [PubMed: 21658579]

Lechan RM, Nestler JL, Jacobson S, Reichlin S. The hypothalamic 'tuberoinfundibular' system of the rat as demonstrated by horseradish peroxidase (HRP) microiontophoresis. Brain Research. 1980; 195:13–27. [PubMed: 7397491]

Lee SJ, Kirigiti M, Lindsley SR, Loche A, Madden CJ, Morrison SF, Smith SM, Grove KL. Efferent projections of neuropeptide Y-expressing neurons of the dorsomedial hypothalamus in chronic hyperphagic models. Journal of Comparative Neurology. 2013; 521:1891–1914. DOI: 10.1002/cne.23265 [PubMed: 23172177]

Lee SJ, Diener K, Kaufman S, Krieger JP, Pettersen KG, Jejelava N, Arnold M, Watts AG, Langhans W. Limiting glucocorticoid secretion increases the anorexigenic properties of Exendin-4. Molecular Metabolism. 2016; 5(7):552–65. DOI: 10.1016/j.molmet.2016.04.008 [PubMed: 27408779]

Légrádi G, Lechan RM. Agouti-related protein containing nerve terminals innervate thyrotropin-releasing hormone neurons in the hypothalamic paraventricular nucleus. Endocrinology. 1999; 140(8):3643–3652. [PubMed: 10433222]

Légrádi G, Hannibal J, Lechan RM. Pituitary adenylate cyclase-activating polypeptide-nerve terminals densely innervate corticotropin-releasing hormone-neurons in the hypothalamic paraventricular nucleus of the rat. Neuroscience Letters. 1998; 246(3):145–148. [PubMed: 9792613]

Li C, Chen P, Smith MS. Corticotropin releasing hormone neurons in the paraventricular nucleus are direct targets for neuropeptide Y neurons in the arcuate nucleus: an anterograde tracing study. Brain Research. 2000; 854(1):122–129. [PubMed: 10784113]

Liposits Z, Phelix C, Paull WK. Electron microscopic analysis of tyrosine hydroxylase, dopamine-β-hydroxylase and phenylethanolamine-N-methyltransferase immunoreactive innervation of the hypothalamic paraventricular nucleus in the rat. Histochemistry. 1986a; 84(2):105–120. [PubMed: 2872191]

Liposits Z, Phelix C, Paull WK. Adrenergic innervation of corticotropin releasing factor (CRF)—synthesizing neurons in the hypothalamic paraventricular nucleus of the rat. Histochemistry. 1986b; 84(3):201–205. [PubMed: 3519543]

Lorang D, Amara SG, Simerly RB. Cell-type-specific expression of catecholamine transporters in the rat brain. Journal of Neuroscience. 1994; 14(8):4903–4914. [PubMed: 8046459]

Martens H, Weston MC, Boulland JL, Gronborg M, Grosche J, Kacza J, Hoffmann A, Matteoli M, Takamori S, Harkany T, Chaudhry FA, Rosenmund C, Erck C, Jahn R, Hartig W. Unique luminal localization of VGAT-C terminus allows for selective labeling of active cortical GABAergic synapses. Journal of Neuroscience. 2008; 28(49):13125–13131. DOI: 10.1523/JNEUROSCI.3887-08.2008 [PubMed: 19052203]

Masliah E, Terry RD, Alford M, DeTeresa R. Quantitative immunohistochemistry of synaptophysin in human neocortex: an alternative method to estimate density of presynaptic terminals in paraffin sections. Journal of Histochemistry and Cytochemistry. 1990; 38(6):837–844. [PubMed: 2110586]

Matsumoto H, Maruyama M, Noguchi J, Horikoshi Y, Fujiwara K, Kitada C, Hinuma S, Onda H, Nishimura O, Inoue K, Fujino M. Stimulation of corticotropin-releasing hormone-mediated adrenocorticotropin secretion by central administration of prolactin-releasing peptide in rats. Neuroscience Letters. 2000; 285(3):234–238. [PubMed: 10806329]

McIntire SL, Reimer RJ, Schuske K, Edwards RH, Jorgensen EM. Identification and characterization of the vesicular GABA transporter. Nature. 1997; 389(6653):870–876. [PubMed: 9349821]

Miklós IH, Kovács KJ. GABAergic innervation of corticotropin-releasing hormone (CRH)-secreting parvocellular neurons and its plasticity as demonstrated by quantitative immunoelectron microscopy. Neuroscience. 2002; 113(3):581–592. [PubMed: 12150778]

Miklós IH, Kovács KJ. Reorganization of synaptic inputs to the hypothalamic paraventricular nucleus during chronic psychogenic stress in rats. Biological Psychiatry. 2012; 71(4):301–308. DOI: 10.1016/j.biopsych.2011.10.027 [PubMed: 22137593]

Mirabella N, Esposito V, Squillacioti C, De Luca A, Paino G. Expression of agouti-related protein (AgRP) in the hypothalamus and adrenal gland of the duck (*Anas platyrhynchos*). Anatomy and Embryology. 2004; 994:267. http://doi.org/10.1007/s00429-004-0431-0.

Münster-Wandowski A, Zander JF, Richter K, Ahnert-Hilger G. Coexistence of functionally different vesicular neurotransmitter transporters. Frontiers in Synaptic Neuroscience. 2016; 8doi: 10.3389/fnsyn.2016.00004

Ni B, Rosteck PR, Nadi NS, Paul SM. Cloning and expression of a cDNA encoding a brain-specific Na(+)-dependent inorganic phosphate cotransporter. Proceedings of the National Academy of Science, USA. 1994; 91(12):5607–5611.

Nilsson I, Lindfors C, Fetissov SO, Hökfelt T, Johansen JE. Aberrant agouti-related protein system in the hypothalamus of theanx/anx mouse is associated with activation of microglia. The Journal of Comparative Neurology. 2007; 507(1):1128–1140. http://doi.org/10.1002/cne.21599.

Ottem EN, Godwin JG, Krishnan S, Petersen SL. Dual-phenotype GABA/glutamate neurons in adult preoptic area: sexual dimorphism and function. Journal of Neuroscience. 2004; 24(37):8097–8105. DOI: 10.1523/JNEUROSCI.2267-04.2004 [PubMed: 15371511]

Pacak K, Palkovits M, Kopin IJ, Goldstein DS. Stress-induced norepinephrine release in the hypothalamic paraventricular nucleus and pituitary-adrenocortical and sympathoadrenal activity: in vivo microdialysis studies. Frontiers in Neuroendocrinology. 1995; 16(2):89–150. [PubMed: 7621982]

Pacak K, Palkovits M, Yadid G, Kvetnansky R, Kopin IJ, Goldstein DS. Heterogeneous neurochemical responses to different stressors: a test of Selye's doctrine of nonspecificity. American Journal of Physiology, Regulatory, Integrative and Comparative Physiology. 1998; 275(4):R1247–R1255.

Pacák K, Palkovits M. Stressor specificity of central neuroendocrine responses: implications for stress-related disorders. Endocrine Reviews. 2001; 22:502–48. [PubMed: 11493581]

Rho JH, Swanson LW. A morphometric analysis of functionally defined subpopulations of neurons in the paraventricular nucleus of the rat with observations on the effects of colchicine. Journal of Neuroscience. 1989; 9(4):1375–88. [PubMed: 2784832]

Rinaman L. Postnatal development of catecholamine inputs to the paraventricular nucleus of the hypothalamus in rats. Journal of Comparative Neurology. 2001; 438(4):411–422. [PubMed: 11559897]

Ritter S, Bugarith K, Dinh TT. Immunotoxic destruction of distinct catecholamine subgroups produces selective impairment of glucoregulatory responses and neuronal activation. Journal of Comparative Neurology. 2001; 432(2):197–216. [PubMed: 11241386]

Ritter S, Li A-J, Wang Q, Dinh TT. Minireview: The value of Looking Backward: The Essential Role of the Hindbrain in Counterregulatory Responses to Glucose Deficit. Endocrinology. 2011; 152(11):4019–4032. DOI: 10.1210/en.2010-1458 [PubMed: 21878511]

Ritter S, Llewellyn-Smith I, Dinh TT. Subgroups of hindbrain catecholamine neurons are selectively activated by 2-deoxy-D-glucose induced metabolic challenge. Brain Research. 1998; 805(1–2):41–54. [PubMed: 9733914]

Ritter S, Watts AG, Dinh TT, Sanchez-Watts G, Pedrow C. Immunotoxin lesion of hypothalamically projecting norepinephrine and epinephrine neurons differentially affects circadian and stressor-stimulated corticosterone secretion. Endocrinology. 2003; 144(4):1357–1367. DOI: 10.1210/en.2002-221076 [PubMed: 12639919]

Rosin DL, Chang DA, Guyenet PG. Afferent and efferent connections of the rat retrotrapezoid nucleus. Journal of Comparative Neurology. 2006; 499(1):64–89. DOI: 10.1002/cne.21105 [PubMed: 16958085]

Santos MS, Li H, Voglmaier SM. Synaptic vesicle protein trafficking at the glutamate synapse. Neuroscience. 2009; 158(1):189–203. DOI: 10.1016/j.neuroscience.2008.03.029 [PubMed: 18472224]

Sarkar J, Wakefield S, MacKenzie G, Moss SJ, Maguire J. Neurosteroidogenesis is required for the physiological response to stress: role of neurosteroid-sensitive GABAA receptors. Journal of Neuroscience. 2011; 31:18198–18210. DOI: 10.1523/JNEUROSCI.2560-11.2011 [PubMed: 22171026]

Sawchenko PE, Swanson LW. The organization of noradrenergic pathways from the brainstem to the paraventricular and supraoptic nuclei in the rat. Brain Research Reviews. 1982; 4(3):275–325.

Sawchenko PE, Swanson LW. The organization of forebrain afferents to the paraventricular and supraoptic nuclei of the rat. Journal of Comparative Neurology. 1983; 218(2):121–144. [PubMed: 6886068]

Sawchenko PE, Swanson LW, Grzanna R, Howe PR, Bloom SR, Polak JM. Colocalization of neuropeptide Y immunoreactivity in brainstem catecholaminergic neurons that project to the paraventricular nucleus of the hypothalamus. Journal of Comparative Neurology. 1985; 241(2):138–153. [PubMed: 3840810]

Seal RP, Edwards RH. Functional implications of neurotransmitter co-release: glutamate and GABA share the load. Current Opinions in Pharmacology. 2006; 6(1):114–119. DOI: 10.1016/j.coph.2005.12.001

Sheng M, Kim E. The postsynaptic organization of synapses. Cold Spring Harbor Perspectives in Biology. 2011; 3(12) pii: a005678. doi: 10.1101/cshperspect.a005678

Simmons DM, Swanson LW. Comparison of the spatial distribution of seven types of neuroendocrine neurons in the rat paraventricular nucleus: toward a global 3D model. Journal of Comparative Neurology. 2009; 516(5):423–41. DOI: 10.1002/cne.22126 [PubMed: 19655400]

Soiza-Reilly M, Commons KG. Quantitative analysis of glutamatergic innervation of the mouse dorsal raphe nucleus using array tomography. Journal of Comparative Neurology. 2011; 519(18):3802–3814. DOI: 10.1002/cne.22734 [PubMed: 21800318]

Somogyi J, Baude A, Omori Y, Shimizu H, Mestikawy SE, Fukaya M, Shigemoto R, Watanabe M, Somogyi P. GABAergic basket cells expressing cholecystokinin contain vesicular glutamate transporter type 3 (VGLUT3) in their synaptic terminals in hippocampus and isocortex of the rat. European Journal of Neuroscience. 2004; 19(3):552–569. [PubMed: 14984406]

Stornetta RL, Sevigny CP, Guyenet PG. Vesicular glutamate transporter DNPI/VGLUT2 mRNA is present in C1 and several other groups of brainstem catecholaminergic neurons. Journal of Comparative Neurology. 2002; 444(3):191–206. DOI: 10.1002/cne.10141 [PubMed: 11840474]

Sved AF. PNMT-containing catecholaminergic neurons are not necessarily adrenergic. Brain Research. 1989; 481(1):113–118. [PubMed: 2706454]

Sved AF. Effect of monoamine oxidase inhibition on catecholamine levels: evidence for synthesis but not storage of epinephrine in rat spinal cord. Brain Research. 1990; 512(2):253–258. [PubMed: 2354362]

Swanson, LW. Brain Maps: Structure of the Rat Brain. 32004. Open access available at http://larrywswanson.com/?page_id164

Swanson LW, Sawchenko PE. Hypothalamic integration: organization of the paraventricular and supraoptic nuclei. Annual Reviews of Neuroscience. 1983; 6(1):269–324.

Swanson LW, Sawchenko PE, Berod A, Hartman BK, Helle KB, Vanorden DE. An immunohistochemical study of the organization of catecholaminergic cells and terminal fields in the paraventricular and supraoptic nuclei of the hypothalamus. Journal of Comparative Neurology. 1981; 196(2):271–285. [PubMed: 6111572]

Thiel G. Synapsin I, synapsin II, and synaptophysin: marker proteins of synaptic vesicles. Brain Pathology. 1993; 3(1):87–95. [PubMed: 7903586]

Tong Q, Ye CP, Jones JE, Elmquist JK, Lowell BB. Synaptic release of GABA by AgRP neurons is required for normal regulation of energy balance. Nature Neuroscience. 2008; 11(9):998–1000. DOI: 10.1038/nn.2167 [PubMed: 19160495]

Tucker DC, Saper CB, Ruggiero DA, Reis DJ. Organization of central adrenergic pathways: I. Relationships of ventrolateral medullary projections to the hypothalamus and spinal cord. Journal of Comparative Neurology. 1987; 259(4):591–603. [PubMed: 2885348]

Vaaga CE, Borisovska M, Westbrook GL. Dual-transmitter neurons: functional implications of co-release and co-transmission. Current Opinion in Neurobiology. 2014; 29:25–32. DOI: 10.1016/j.conb.2014.04.010 [PubMed: 24816154]

van den Pol AN, Wuarin JP, Dudek FE. Glutamate, the dominant excitatory transmitter in neuroendocrine regulation. Science. 1990; 250(4985):1276–1279. [PubMed: 1978759]

Wamsteeker JI, Bains JS. A synaptocentric view of the neuroendocrine response to stress. European Journal of Neuroscience. 2010; 32(12):2011–2021. [PubMed: 21143656]

Wamsteeker Cusulin JI, Füzesi T, Watts AG, Bains JS. Characterization of corticotropin-releasing hormone neurons in the paraventricular nucleus of the hypothalamus of Crh-IRES-Cre mutant mice. PLoS One. 2013; 8(5):e64943.doi: 10.1371/journal.pone.0064943 [PubMed: 23724107]

Watts AG. Glucocorticoid regulation of peptide genes in neuroendocrine CRH neurons: a complexity beyond negative feedback. Frontiers in Neuroendocrinology. 2005; 26(3–4):109–130. DOI: 10.1016/j.yfrne.2005.09.001 [PubMed: 16289311]

Watts AG, Sanchez-Watts G. Interactions between heterotypic stressors and corticosterone reveal integrative mechanisms for controlling corticotropin-releasing hormone gene expression in the rat paraventricular nucleus. Journal of Neuroscience. 2002; 22:6282–9. 20026629. [PubMed: 12122087]

Watts AG, Khan AM. Identifying links in the chain: the dynamic coupling of catecholamines, peptide synthesis, and peptide release in hypothalamic neuroendocrine neurons. Advances in Pharmacology. 2013; 68:421–444. DOI: 10.1016/B978-0-12-411512-5.00020-8 [PubMed: 24054156]

Wiedenmann B, Franke WW. Identification and localization of synaptophysin, an integral membrane glycoprotein of Mr 38,000 characteristic of presynaptic vesicles. Cell. 1985; 41(3):1017–1028. [PubMed: 3924408]

Wiegand SJ, Price JL. Cells of origin of the afferent fibers to the median eminence in the rat. Journal of Comparative Neurology. 1980; 192:1–19. [PubMed: 7410605]

Wittmann G, Lechan RM, Liposits Z, Fekete C. Glutamatergic innervation of corticotropin-releasing hormone-and thyrotropin-releasing hormone-synthesizing neurons in the hypothalamic paraventricular nucleus of the rat. Brain Research. 2005; 1039(1):53–62. DOI: 10.1016/j.brainres.2005.01.090 [PubMed: 15781046]

Wuarin JP, Dudek FE. Excitatory amino acid antagonists inhibit synaptic responses in the guinea pig hypothalamic paraventricular nucleus. Journal of Neurophysiology. 1991; 65(4):946–951. [PubMed: 1675675]

Yang JH, Li LH, Lee S, Jo IH, Lee SY, Ryu PD. Effects of adrenalectomy on the excitability of neurosecretory parvocellular neurones in the hypothalamic paraventricular nucleus. Journal of Neuroendocrinology. 2007; 19(4):293–301. DOI: 10.1111/j.1365-2826.2007.01531.x [PubMed: 17355319]

Yang JH, Li LH, Shin SY, Lee S, Lee SY, Han SK, Ryu PD. Adrenalectomy potentiates noradrenergic suppression of GABAergic transmission in parvocellular neurosecretory neurons of hypothalamic paraventricular nucleus. Journal of Neurophysiology. 2008; 99(2):514–523. DOI: 10.1152/jn.00568.2007 [PubMed: 18032568]

Yoon YS, Lee JS, Lee HS. Retrograde study of CART-or NPY-neuronal projection from the hypothalamic arcuate nucleus to the dorsal raphe and/or the locus coeruleus in the rat. Brain Research. 2013; 1519:40–52. doi.org/10.1016/j.brainres.2013.04.039. [PubMed: 23628478]

Zander JF, Munster-Wandowski A, Brunk I, Pahner I, Gomez-Lira G, Heinemann U, Gutierrez R, Laube G, Ahnert-Hilger G. Synaptic and vesicular coexistence of VGLUT and VGAT in selected

excitatory and inhibitory synapses. Journal of Neuroscience. 2010; 30(22):7634–7645. DOI: 10.1523/JNEUROSCI.0141-10.2010 [PubMed: 20519538]

Zheng H, Stornetta RL, Agassandian K, Rinaman L. Glutamatergic phenotype of glucagon-like peptide 1 neurons in the caudal nucleus of the solitary tract in rats. Brain Structure and Function. 2015; 220(5):3011–3022. DOI: 10.1007/s00429-014-0841-6 [PubMed: 25012114]

Ziegler DR, Herman JP. Local integration of glutamate signaling in the hypothalamic paraventricular region: regulation of glucocorticoid stress responses. Endocrinology. 2000; 141(12):4801–4804. [PubMed: 11108297]

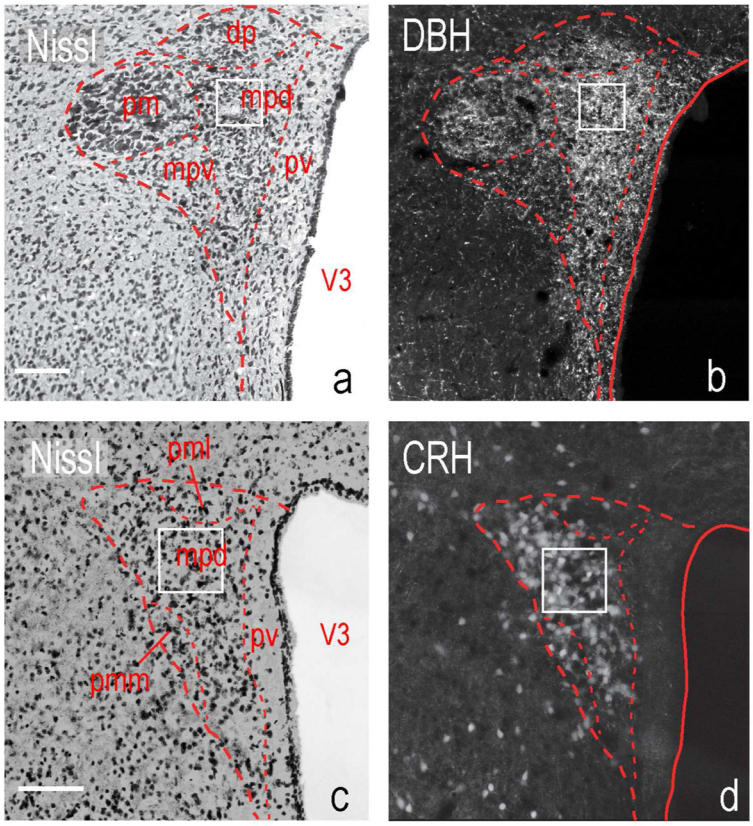

Figure 1. The rat and mouse paraventricular nucleus of the hypothalamus (PVH)

Thionin-stained sections containing (a) the rat PVH at level 26 of Swanson [2004], and (c) mouse PVH at level P56, Image 61 of Dong [2007] (Also see Biag et al., [2012]). Appropriate serial sections show either immunostaining for DBH (b, rat) or endogenous td-Tomato fluorescence in a ***Crh-IRES-Cre;Ai14*** mouse (d). White boxes indicate the sampling region for all images. Scale bars indicate 100μm. Abbreviations: dp, dorsal parvicellular part; mpd, medial parvicellular part, dorsal zone; mpv, medial parvicellular part, ventral zone; pm, posterior magnocellular part; pv, periventricular part; V3, third ventricle.

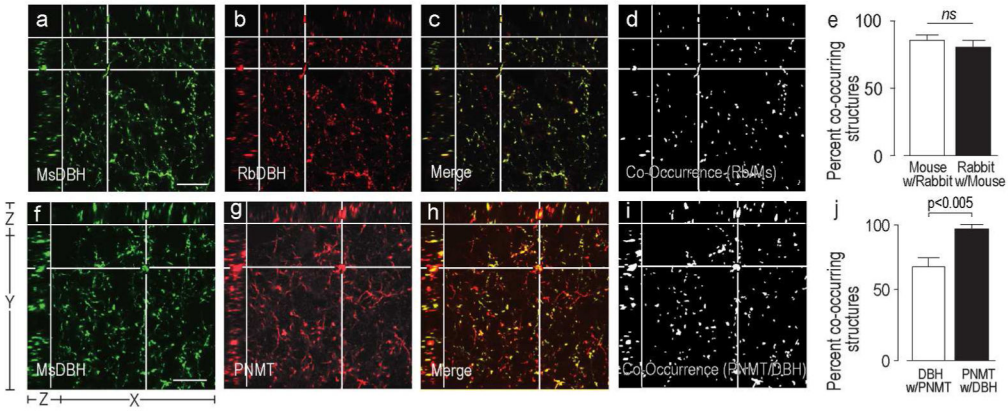

Figure 2. Validation of Image Analytical Methods

Three plane orthogonal views obtained from confocal Z-stacks of part of the rat PVHmpd. The arrangement of the X, Y, and Z planes are shown on panel a. The XY part of each panel shows the uppermost image of each Z-stack. The images show the degree of co-occurrence of structures immunostained with either a mouse monoclonal DBH antibody and a rabbit polyclonal DBH antibody DBH (a–d), or a mouse monoclonal DBH antibody and a rabbit polyclonal PNMT antibody (f–i). Panels a), b), f), and g) show structures stained with the individual antibodies. Panels c) and h) are the respective merged images where single labeled structures are in red or green and co-occurring structures in yellow. Panels d) and i) show any structure that contained labeling from both antibodies (white) extracted from panels c) and h), respectively. The horizontal and vertical white lines in panels a)–d) and f)–i) target a representative double-labeled structures in the X, Y, and Z planes. There is no significant difference between the percent co-occurrence of the structures labeled with the two DBH antibodies (e). However, because all PNMT always co-occurs with DBH but not all DBH occurs with PNMT there was a significant difference between the percent co-occurrence of the two antigens depending on which one was considered the reference antigen (j). Error bars in e) and j) indicate mean + S.E.M. Scale bar represents 20μm.

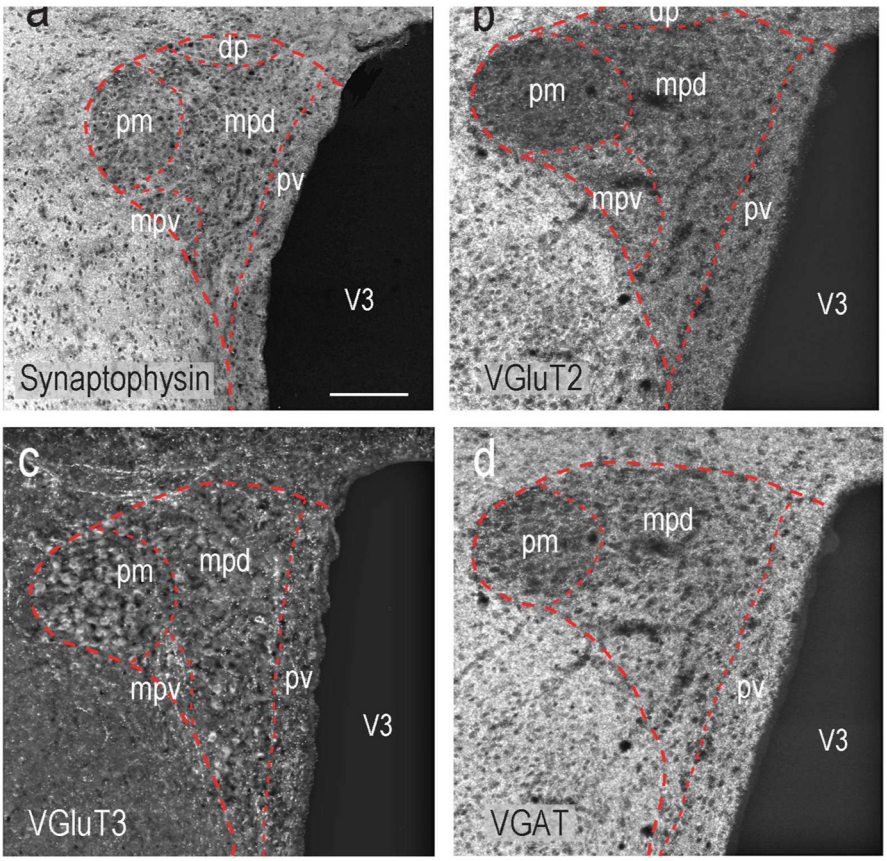

Figure 3. Glutamatergic and GABAergic Innervation Patterns of the rat and mouse PVH

The locations of synaptophysin (a) VGluT2 (b), VGluT3 (c), and VGAT (d) immunolabeled structures in the rat PVH and adjacent regions. Note that peri-PVH regions have significantly higher levels of VGluT2 and VGAT that the PVH itself. Abbreviations as Figure 2. Scale bar represents 150μm.

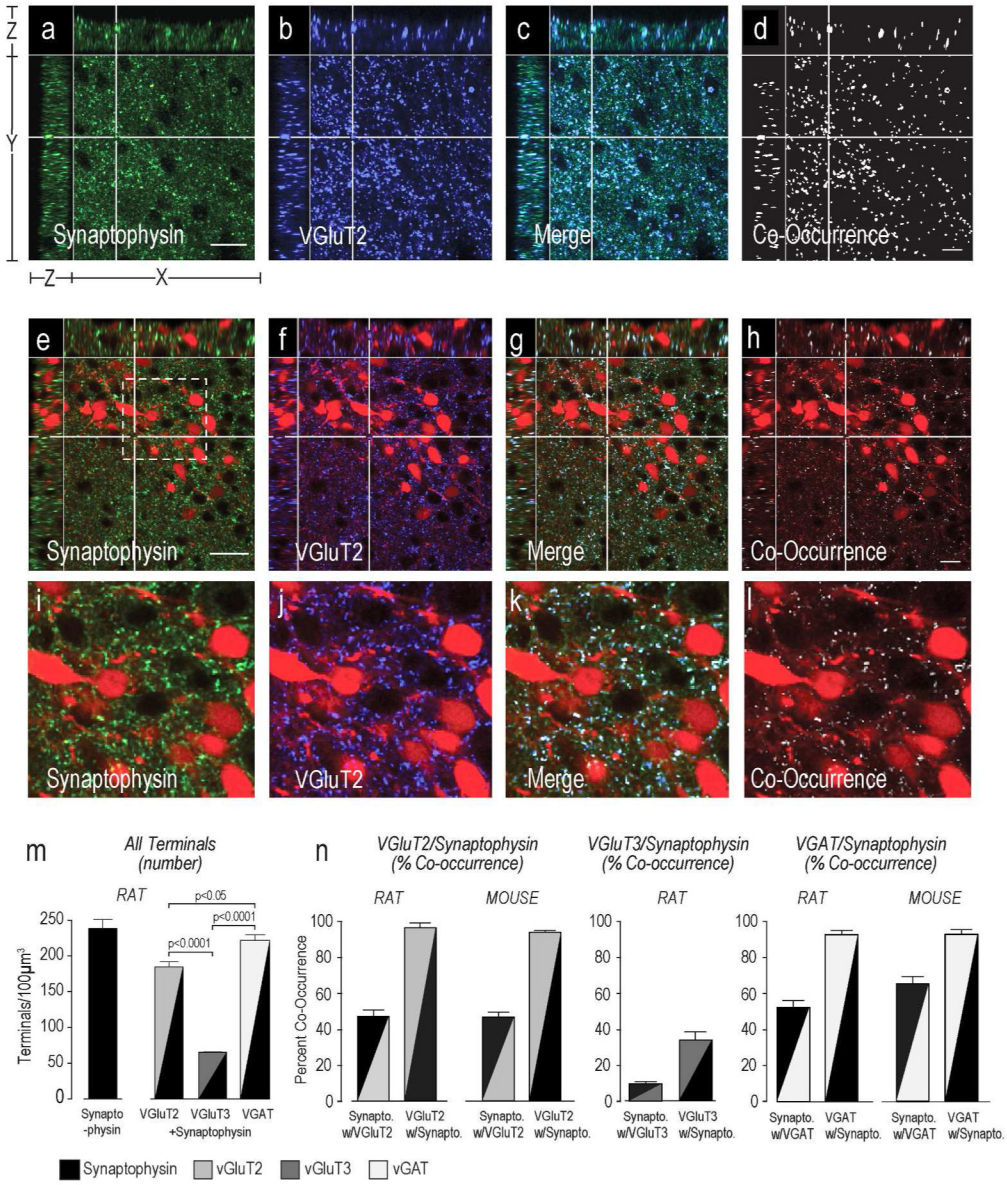

Figure 4. VGluT2 and VGAT, but not VGluT3 are Expressed Exclusively in Pre-Synaptic

Terminals Synaptophysin (a,e,i), VGluT2 (b,f,j), and terminals labeled with both molecules (c,d, g,h, and k,l) in the rat (a–d) and mouse (e–l) PVHmpd (see Fig. 1 for orientation). TdTomato-labeled CRH soma are visible in the mouse panels. Equivalent images are not shown for VGAT or VGluT3. Please see Figure 2 for more information about the general organization of the confocal image panels. Panels i-l show higher magnification images of the area indicated by the dashed line square in e. Scale bar in a) and e) indicates 20µm for panels a – h. Scale bar in i indicates 100em. All VGluT2 and VGAT occurs in rat and mouse (female) pre-synaptic terminals (m,n), but not not all VGluT3 occurs in rat pre-synaptic terminals (m,n). There are significantly more VGAT presynaptic terminals than either Glu transporters, and significantly more VGluT2 than VGluT3 terminals (n). Error bars represent the mean + S.E.M.

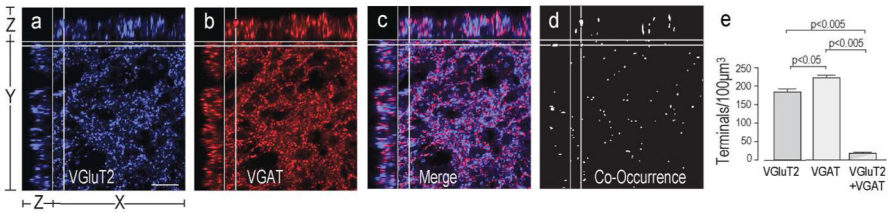

Figure 5. VGluT2 and VGAT Co-Occur in a Population of Terminals in the Rat PVHmpd

VGluT2 (a) and VGAT (b) co-occur in some terminals (c–e) in the rat PVHmpd. Please see Figure 2 for more information about the general organization of the confocal image panels. There are significantly fewer terminals containing both vesicular transporters than terminals containing only one transporter (e). Scale bar indicates 20μm. Error bars represent mean + S.E.M.

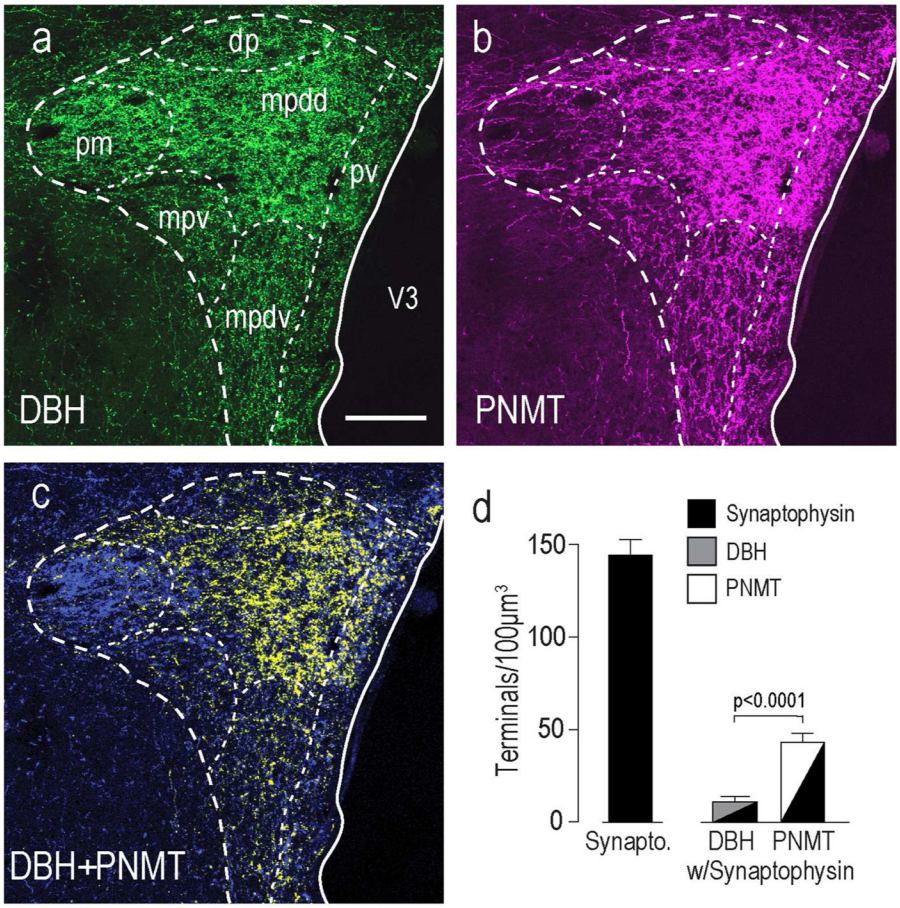

Figure 6. Catecholaminergic Innervation to the PVH

DBH (a) and PNMT (b) immunoreactivity in the rat PVH and its surrounding regions. Panel c) is a merge of a) and b) to show co-occurring DBH and PNMT structures and DBH-only structures. Within the PVHmpdd there are significantly more PNMT than DBH- only structures (c). Scale bar is 150μm for all panels. Abbreviations are as Figure 1 except for: mpdd, medial parvicellular part, dorsal zone (dorsal division); mpdv, medial parvicellular part, dorsal zone (ventral division). Panel d) shows that there were significantly more PMNT-containing presynaptic terminals in the PVHmpd than those containing DBH-only (no confocal images are shown for these results). Error bars indicate mean + S.E.M.

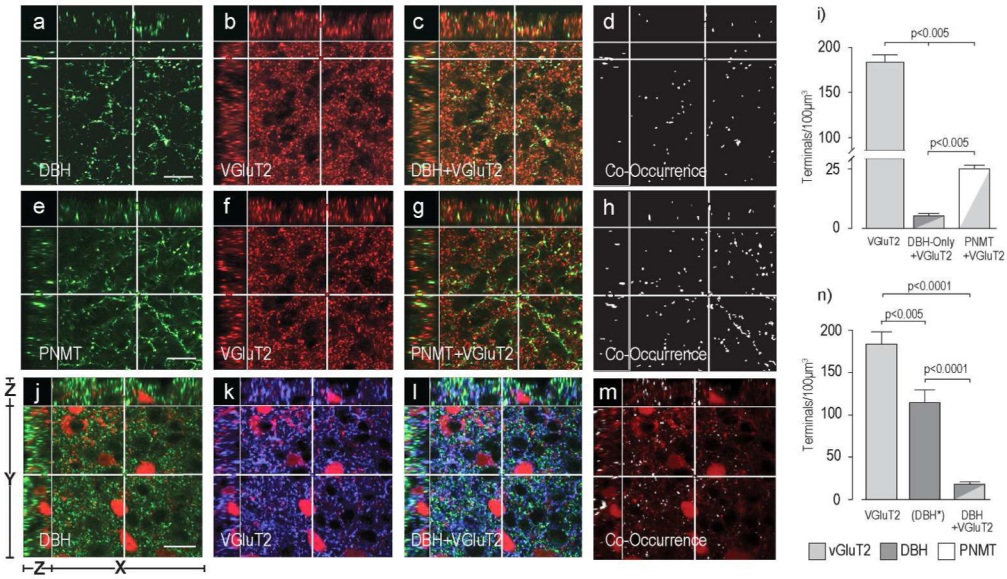

Figure 7. Some Catecholamine Terminals in the PVHmpd of the Rat and Mouse Express VGluT2

Panels a) – h) show DBH-ir (a–d) or PNMT-ir (e–h) in the rat PVHmpd together with VGluT2-ir (b,f) and its co-occurrence with DBH (c,d) or PNMT (g,h). There are significantly more PNMT than DBH-only terminals that also contain VGluT2 in the rat PVHmpd (i). Please note the change in the scale of the Y axis in panel i). Panels j) – m) show DBH-ir (j) and VGluT2-ir (k) in the female mouse PVHmpd. TdTomato-labeled CRH soma can be seen in panels j) – m). The co-occurrence of DBH and VGluT2 is shown in l) and m). Scale bar indicates 20µm for all panels. Note that in panel n) the (DBH*) data are DBH-immunoreactive structures only. Group data in n) are from female mice. Because of species incompatibility there was no synaptophysin labeling in this experiment to verify that non-VGluT2-ir DBH structures were terminals. Scale bar indicates 20µm for all image panels. Please see Figure 2 for more information about the general organization of the confocal image panels. Error bars indicate mean + S.E.M.

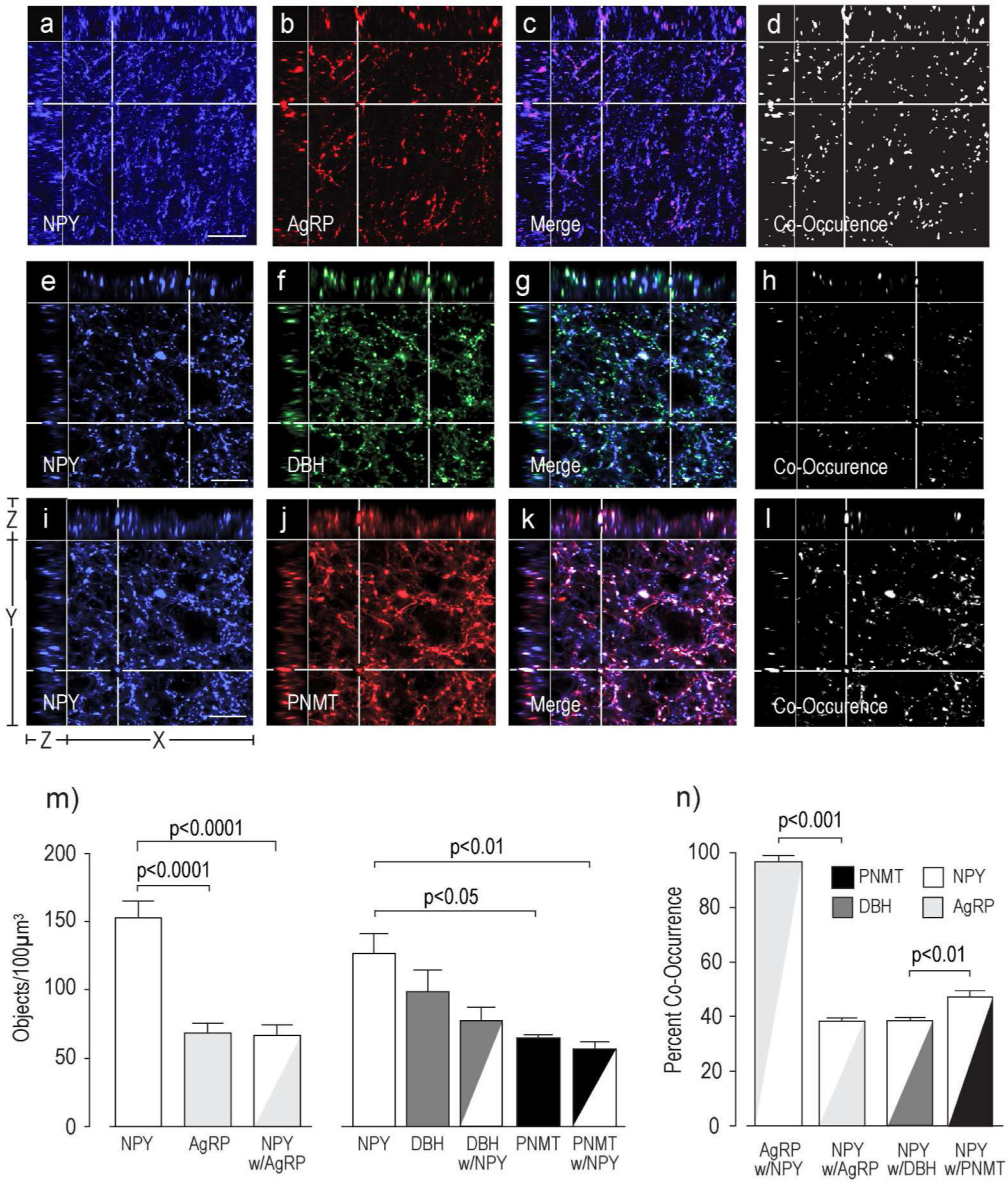

Figure 8. Co-Occurrence of NPY with AgRP, DBH, or PNMT

Panels a) – l) show NPY-ir with AgRP-ir (a–d), NPY with DBH-ir only (e-h), or NPY with PNMT-ir only (i–l) in the rat PVHmpd. Co-occurring structures (c,d, g,h, k,l) were identified and counted (m), together with their percent co-occurrence (n). Please see Figure 2 for more information about the general organization of the confocal image panels. Scale bars indicates 20µm. Error bars indicate mean + S.E.M.

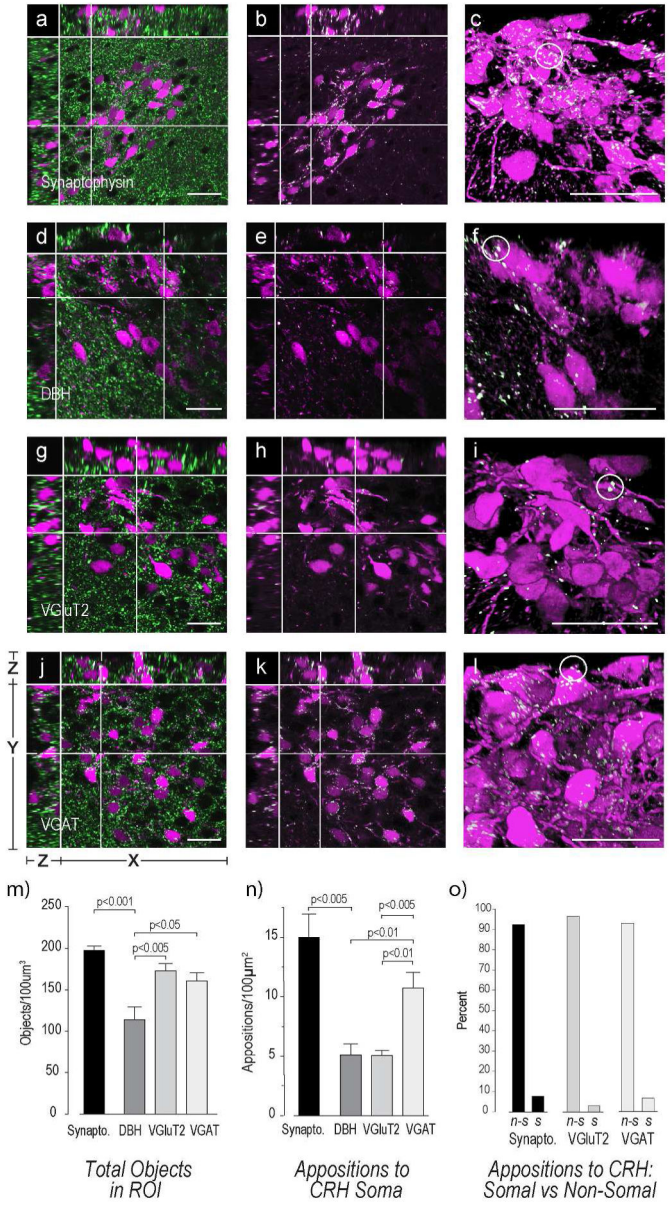

Figure 9. Appositions to CRH Neurons in the Mouse PVHmpd

Female mouse sections containing the PVHmpd were labeled with antibodies against synaptophysin (a–c), DBH (d–f), VGluT2 (g–i), and VGAT (j–l) and analyzed for appositions of each type against the soma of the CRH neuron. Please see Figure 2 for more information about the general organization of the confocal image panels. The white structures in all confocal images except a) d), g), and j) are those that are double-labeled and fulfill the apposition criterion established by Bouyer & Simerly [2013]. See Methods for more details. Images c), f), i), and l) are 3D renderings of the Z-stacks used for images b), e), h), and k), respectively. White circles highlight some somatic appositions. There are significantly more VGAT and VGluT2 terminals than DBH terminals (m). However, VGAT somatic appositions are more numerous than either VGluT2 or DBH (n). There are significantly more appositions to the non-somatic regions of the CRH neuron (o). Group

data in m) – n) are from female mice. Abbreviations for o): n-s, non-somatic; s, somatic. Scale bars indicate 20μm. Error bars indicate mean + S.E.M.

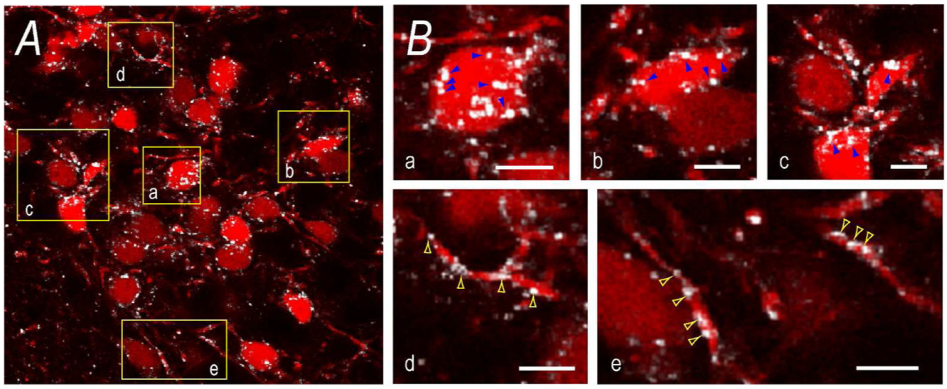

Figure 10. Appositions to CRH Neurons in the Mouse PVHmpd

Panel A) is panel e) from Figure 9. It shows VGAT appositions (white) to TdTomato-labeled CRH soma. To highlight somatic and non-somatic appositions, panel B) shows magnified regions (yellow boxes) from A). Blue arrows in a), b), and c) indicate some VGAT appositions to CRH soma. Yellow arrows in d) and e) indicate some VGAT appositions to non-somatic regions, presumably dendrites. Scale bars represent 20μm in A), and 5μm in B).

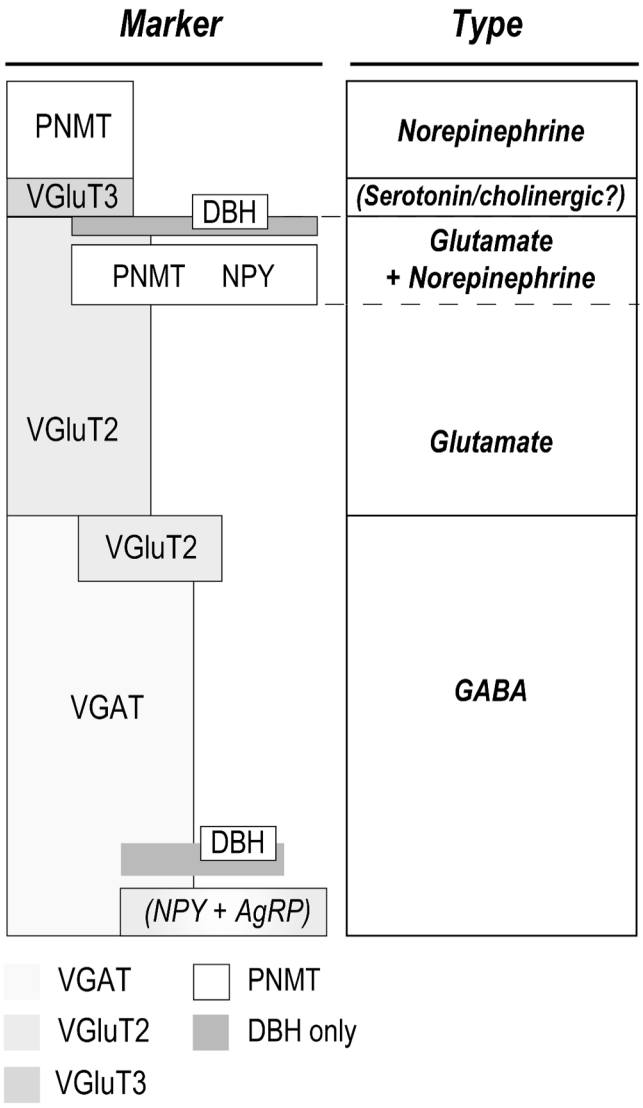

Figure 11. Pre-Synaptic Terminal Diversity in the Rat PVHmpd

Figure 11 summarizes two sets of relationships in pre-synaptic terminals identified in the rat PVHmpd in the absence of stressors:

1) ***Marker***. The height of each box approximates the proportion of that marker to the total number of synaptophysin-labeled pre-synaptic terminals. Overlapping boxes indicate co-occurrence between two markers. While we did not investigate the co-occurrence of VGAT with NPY, the majority of NPY innervation co-occurs with catecholaminergic (and particularly PNMT-containing afferents. The remainder originated from hypothalamic sources [Bai et al., 1985; Sawchenko et al., 1985; Füzesi et al., 2007]. NPY originating from the arcuate nucleus co-occurs with AgRP, the majority of which is GABAergic [Tong et al., 2008]. While we did not investigate serotonergic or cholinergic inputs, evidence indicates that serotonergic inputs originate from hindbrain raphe neurons that contain VGluT3 [Gras et al., 2002; Herzog et al., 2004].

2) ***Type*** The presumed major signaling molecule.

Abbreviations: AgRP, agouti-related peptide; DBH, dopamine β-hydroxylase; αMSH, NPY, neuropeptide Y; PNMT, phenylethanolamine N-methyltransferase; VGAT, vesicular GABA transporter; VGlut2, vesicular glutamate transporter 2; VGlut3, vesicular glutamate transporter 3.

TABLE 1

Primary Antibody	Immunogen	Supplier	Number Catalogue	RRID	Titer
Rabbit anti-Agouti Related Peptide	Synthetic peptide sequence N'-TRSCPNMATGRCYCFANFFR CACPDCCPVQQGSEHLRVCRRSS- C' (Human)	Phoenix Pharmaceuticals	H-003-53	AB_2313908	1:5,000
Mouse anti-Dopamine-β-Hydroxylase	Purified bovine DBH	EMD Millipore	MAB308	AB_2245740	1:20,000
Rabbit anti-Dopamine-β-Hydroxylase	Bovine DBH	ImmunoStar	22806	AB_572229	1:2,000
Sheep anti-Neuropeptide Y	Synthetic NPY peptide conjugated to bovine thyroglobulin	EMD Millipore	AB1583	AB_2236176	1:5,000
Rabbit anti- Phenylethanolamine N-Methyltransferase	Purified PNMT enzyme from rabbit adrenal medulla	Dr. M. Bohn, Northwestern University	N/A	AB_2315181	1:10,000
Goat anti-Synaptophysin	E. coli-derived recombinant human synaptophysin	R&D Systems	AF5555	AB_2198864	1:5,000
Rabbit anti-Vesicular GABA Transporter	Synthetic peptide AEPPVEGDIHYQR (aa 75 – 87 in rat) coupled to KLH	Synaptic Systems	131 002	AB_887871	1:20,000
Guinea Pig anti-Vesicular Glutamate Transporter 2	KLH-conjugated linear peptide corresponding to amino acids 501- 582 (cytoplasmic C-terminus) of rat VGlut2.	EMD Millipore	AB2251	AB_1587626	1:10,000
Guinea Pig anti-Vesicular Glutamate Transporter 3	Fusion protein amino acids 546–588 (cytoplasmic C-terminus) of rat VGlut3.	EMD Millipore	AB5421	AB_2187832	1:10,000

TABLE 2

Secondary Antibody	Supplier	Catalogue Number	RRID	Titer
AffiniPure Donkey anti-Mouse IgG (H+L) Alexa 488	Jackson ImmunoResearch	715-545-151	AB_2341099	1: 2,000
AffiniPure Donkey anti-Rabbit IgG (H+L) Alexa 488	Jackson ImmunoResearch	711-545-152	AB_2313584	1: 2,000
AffiniPure Donkey anti-Goat IgG (H+L) Cy3	Jackson ImmunoResearch	705-165-147	AB_2307351	1: 2,000
AffiniPure Donkey anti-Rabbit IgG (H+L) Cy3	Jackson ImmunoResearch	711-165-152	AB_2307443	1: 2,000
AffiniPure Donkey anti-Guinea Pig IgG (H+L) Alexa 647	Jackson ImmunoResearch	706-605-148	AB_2340476	1: 2,000
AffiniPure Donkey anti-Sheep IgG (H+L) Alexa 647	Jackson ImmunoResearch	713-605-003	AB_2340750	1: 2,000